On the Heterogeneous Nature of Cisplatin-1-Methyluracil Complexes: Coexistence of Different Aggregation Modes and Partial Loss of NH_3 Ligands as Likely Explanation

Sonja Pullen,*[a] Alexander Hegmans,[a] Wolf G. Hiller,[a] André Platzek,[a] Eva Freisinger,*[a, b] and Bernhard Lippert*[a]

The conversion of the 1:1-complex of Cisplatin with 1-methyluracil (1MeUH), *cis*-[Pt(NH_3)$_2$(1MeU-*N3*)Cl] (**1 a**) to the aqua species *cis*-[Pt(NH_3)$_2$(1MeU-*N3*)(OH_2)]$^+$ (**1 b**), achieved by reaction of **1 a** with $AgNO_3$ in water, affords a mixture of compounds, the composition of which strongly depends on sample history. The complexity stems from variations in condensation patterns and partial loss of NH_3 ligands. In dilute aqueous solution, **1 a**, and dinuclear compounds *cis*-[(NH_3)$_2$(1MeU-*N3*)Pt(μ-OH)Pt(1MeU-*N3*)(NH_3)$_2$]$^+$(**3**) as well as *head-tail cis*-[Pt$_2$(NH_3)$_4$(μ-1MeU-*N3,O4*)$_2$]$^{2+}$ (**4**) represent the major components. In addition, there are numerous other species present in minor quantities, which differ in metal nuclearity, stoichiometry, stereoisomerism, and Pt oxidation state, as revealed by a combination of ^{1}H NMR and ESI-MS spectroscopy. Their composition appears not to be the consequence of a *unique and repeating* coordination pattern of the 1MeU ligand in oligomers but rather *the coexistence of distinctly different condensation patterns*, which include μ-OH, μ-1MeU, and μ-NH_2 bridging and combinations thereof. Consequently, the products obtained should, in total, be defined as a heterogeneous mixture rather than a mixture of oligomers of different sizes. In addition, a N_2 complex, [Pt(NH_3)(1MeU)(N_2)]$^+$ appears to be formed in gas phase during the ESI-MS experiment. In the presence of Na^+ ions, multimers *n* of **1 a** with *n* = 2, 3, 4 are formed that represent analogues of non-metalated uracil quartets found in tetrastranded RNA.

1. Introduction

There is probably no more appropriate introduction to this manuscript than a statement made in a review dealing with preparative methods of platinum antitumor complexes, namely that "the complexity of many seemingly simple reactions of platinum compounds… can be deceptively complicated".[1] As we will show, this applies also to the simple model nucleobase compound, *cis*-[Pt(NH_3)$_2$(1MeU-*N3*)Cl]·H_2O (with 1MeU = 1-methyluracil anion), and its conversion to the corresponding aqua species following treatment with $AgNO_3$. The removal of halide ligands from Pt^{II}complexes by means of a silver salt is a common procedure employed in preparative Pt chemistry. In earlier reports on related simple complexes with 1-methylcytosine (1MeC)[2] as well as 1-methyluracil ligands[3,4] we have provided ample evidence how true the above statement can be. Besides the planned and expected main products in seemingly straightforward reactions also a multitude of minor products are formed, which in large part remain poorly characterized or not characterized at all. In a way it seems funny that, despite the occurrence of minor side products in the low-percent regime, some striking features such as an intense color, can coin the name of a whole class of compounds. This applies, for example, to the so-called "Platinum Pyrimidine Blues", which are obtained by the reaction of the diaqua species of the anticancer agent Cisplatin, *cis*-[Pt(NH_3)$_2$$Cl_2$], with pyrimidine nucleobases or related cyclic amides.[5] It is also true for the classical "Platinblau"[6] and the "Platinum Acetate Blue"[7], which represent amorphous materials and are formed side by side with well-characterized, crystalline products, yet frequently coloring the latter. Over the years, while applying a large number of different ligands, essential features of some of these materials have been recognized, such as multi-nuclearity, stacking of dinuclear building blocks, and mixed-valency.[8,9] However, there is every reason to believe that alternative association patterns, different from the established ones and likewise giving rise to intensely colored materials, exist. For example, with bridging pyrazolate a deep-blue cyclic trinuclear complex with formal Pt^{III}Pt^{III}Pt^{II}oxidation states has been described.[10] Even mononuclear Pt complexes can display "dark blue, almost black" colors.[11]

[a] Dr. S. Pullen, Dr. A. Hegmans, Prof. W. G. Hiller, A. Platzek, Prof. E. Freisinger, Prof. B. Lippert
Fakultät Chemie und Chemische Biologie (CCB)
Technische Universität Dortmund
Otto-Hahn-Str. 6
44221 Dortmund (Germany)
E-mail: sonja.pullen@tu-dortmund.de
freisinger@chem.uzh.ch
bernhard.lippert@tu-dortmund.de
[b] Prof. E. Freisinger
Department of Chemistry
University of Zurich
Winterthurerstrasse 190
8057 Zurich (Switzerland)

Supporting information for this article is available on the WWW under https://doi.org/10.1002/open.202000317

At the outset of the present study we were interested in rationalizing the nature of a "Pt blue" derived from the 1:1-complex *cis*-[Pt(NH_3)$_2$(1MeU-*N3*)(H_2O)](NO_3) with the premise of finding a single and unique coordination pattern responsible for its properties. We failed in reaching this goal, but instead realized how important the "sample history" is, hence the way the reaction mixture is worked up, and that different ways of aggregation and/or condensation of mononuclear species co-exist. Furthermore, we found that the abstraction of AgCl during formation of the Pt-aqua species is anything but "clean" to the extent generally believed, and that NH_3 ligands are partially liberated. We note that some of these "problems", as evident from elemental analysis data of main or side products of "Pt blues" or the presence of Ag^+, have been recognized before.[8a,b] In the following, and if appropriate, we occasionally refer to structural evidence with compounds of Pt^{II} (and of Pd^{II}) having two closely related pyrimidine model nucleobases, namely 1-methylthymine (1MeTH) and 1-methylcytosine (1MeC) (Scheme 1).[12]

2. Results and Discussion

2.1. Formation and Characterization of *cis*-[Pt(NH_3)$_2$(1MeU-*N3*)Cl]·H_2O (1 a) and *cis*-[Pt(NH_3)$_2$(1MeU-*N3*)I] (1a')

The title compound used in the present study, *cis*-[Pt(NH_3)$_2$(1MeU-*N3*)Cl]·H_2O (**1 a**), has been prepared in a "detour" way by first synthesizing *cis*-[Pt(NH_3)$_2$(1MeU-*N3*)$_2$] (**2**] and subsequent removal of one of the two 1MeU ligands by addition of HCl.[13] This procedure involves the transient formation of a protonated 1-methyluracilato ligand, hence of a rare tautomer of 1MeUH, which is then expelled from the starting compound and instantaneously converts to the preferred dioxo tautomer of 1MeUH.[14] Chloride then coordinates to Pt. In our hands, this procedure led to fewer side products than a direct reaction of *cis*-[Pt(NH_3)$_2$Cl$_2$] with 1MeUH. Earlier we had prepared the 1MeT analogue (1MeT = 1-methylthymine anion) in an analogous way and characterized the product by X-ray analysis.[15] Replacement of the chloride ligand in **1 a** by iodide gives poorly water-soluble yellow crystals of *cis*-[Pt(NH_3)$_2$(1MeU-*N3*)I] (**1 a'**), for which likewise an X-ray analysis had been undertaken (Figure 1).

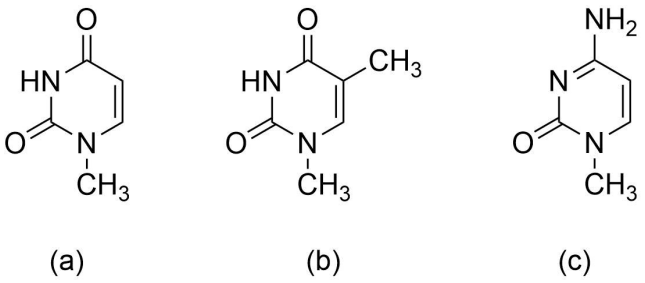

Scheme 1. Structures of (a) 1-methyluracil (1MeUH), and related model nucleobases 1-methylthymine (1MeTH) (b), and 1-methylcytosine (1MeC) (c).

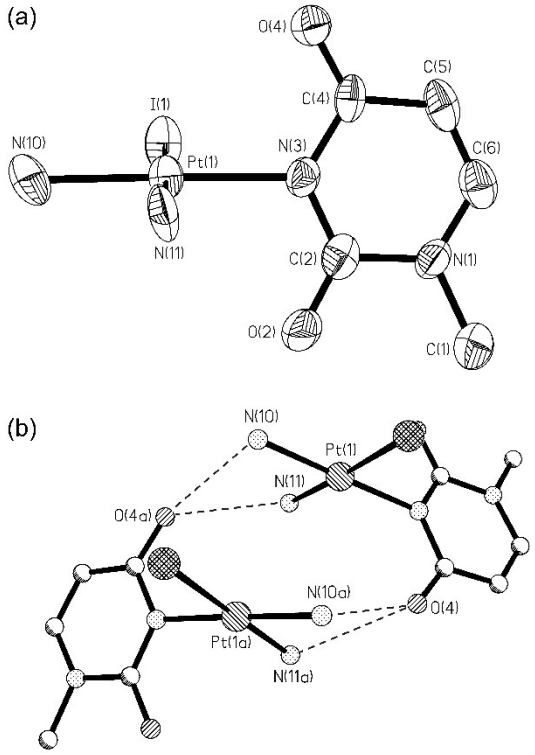

Figure 1. (a) View of *cis*-[Pt(NH_3)$_2$(1MeU-*N3*)I] (**1 a'**) with atom numbering scheme. Ellipsoids are drawn at the 50% probability level. (b) Hydrogen bonded dimer with symmetry related molecule (−x+1, +y, −z+0.5).

1 a' reveals no unusual structural features: As expected, the Pt-NH_3 bond trans to iodide is significantly longer (2.104(7) Å) than the Pt-NH_3 bond trans to N3 of 1MeU (2.050(8) Å) and the metal ion adopts a square-planar coordination geometry. Bond angles and bond distances are normal. Within the crystal lattice, dimers are formed via hydrogen bonds between the two ammonia ligands of one to the 1MeU–O4 group of a second, symmetry-related complex (−x+1, +y, −z+0.5; 2.87(1) and 2.95(1) Å). This interaction causes a large dihedral angle (77.7(3)°) between the 1MeU plane and the Pt coordination plane within one molecule. Additional interactions involving the ammine ligands and O2 groups of further molecules lead to an extensive hydrogen bond network. For more structural details see the Supporting Information (Table S1 and Figure S1).

1 a precipitates in the form of colorless microneedles from water. Minor impurities, originating from the procedure of preparation are removed by brief washing with DMF (*cis*-[Pt(NH_3)$_2$Cl$_2$]) and stirring with excess MeOH (1MeUH). According to elemental analysis and IR spectroscopy (no bands due to 1MeUH and Cisplatin present) the so obtained product is "pure". However, ^{1}H NMR spectroscopy (D_2O, 500 or 600 MHz) in most cases reveals minute impurities of the starting material **2** (ca. 0.1–2%) and also of 1MeUH (0–1.3%), yet neither of DMF nor of MeOH. The amounts of these impurities can conveniently be determined by comparing the integrated intensities of these impurities with the intensities of the ^{13}C satellites of the methyl resonance of the 1MeU ligand in **1 a**, which are 0.5% each (^1J =

140 Hz) (Figure S2). Table 1 lists the Pt species discussed in this paper.

2.2. Solution Behavior of 1 a in D_2O

When dissolved in D_2O, the ^1H NMR spectrum of **1 a** reveals the expected H6 and H5 doublets ($^3J = 7.44$ Hz) and a singlet for the methyl group at 7.41, 5.67, and 3.35 ppm, respectively.[4] The H5 signal is shown in Figure 2 (a)).

With time (days – weeks; sample at room temperature and in the dark), new resonances grow in (Figure 2 (b)). Only H5 doublets are depicted as these are better dispersed than their H6 counterparts. Their chemical shifts are clearly in the regions typical of terminal 1MeU-*N3* ligands bound to Pt^{II}[4] and rule out the presence of μ-1MeU species to any detectable amount under these conditions (**1 a** kept at room temperature, pD eventually 7.5). μ-1MeU ligands typically have their H5 protons at chemical shifts >5.86 ppm. Not counting the mentioned possible impurities, at least four new sets of resonances emerge

Table 1. Species discussed in this paper.

1a	*cis*-$[Pt(NH_3)_2(1MeU\text{-}N3)Cl]*H_2O$
1a'	*cis*-$[Pt(NH_3)_2(1MeU\text{-}N3)I]$
1b	*cis*-$[Pt(NH_3)_2(1MeU\text{-}N3)(OH_2)]^+$
1c	*trans*-$[Pt(NH_3)(1MeU\text{-}N3)Cl_2]^-$
1d	$[PtCl(OH_2)(1MeU\text{-}N3)(NH_3)]$ (SP-4-2)
1e	*trans*-$[Pt(NH_3)(1MeU\text{-}N3)(OH_2)_2]^+$
2	*cis*-$[Pt(NH_3)_2(1MeU\text{-}N3)_2]*4H_2O$
2a	*cis*-$\{[Pt(NH_3)_2(1MeU\text{-}N3)_2]Ag_x\}^{x+}$
3	*cis*-$[(NH_3)_2(1MeU\text{-}N3)Pt(\mu\text{-}OH)Pt(1MeU\text{-}N3)(NH_3)_2]^+$
4	*head-tail cis*-$[Pt_2(NH_3)_4(1MeU\text{-}N3,O4)_2]^{2+}$
5	*head-head cis*-$[Pt_2(NH_3)_4(1MeU\text{-}N3,O4)_2]^{2+}$
6	linear Pt_3 species
7	hydrolysis product of 1c, possibly 1d or 1e
8	*cis*-$[(NH_3)_2Pt(\mu\text{-}OH)(\mu\text{-}1MeU\text{-}N3,O4)Pt(NH_3)_2]^{2+}$
X	Pt^{IV} complex with unclear composition
Y	complex with Pt at N3 and O4, with mutual "face-back" orientation
9	*trans*-$Cs[Pt(NH_3)(1MeU\text{–}N3)I_2]*H_2O$
10	$[Pt(NH_3)_4][trans\text{-}Pt(NH_3)(1MeU\text{—}N3)I_2]_2*5H_2O$
11	*trans*-$[Pt(NH_3)(DMSO\text{–}S)I_2]$

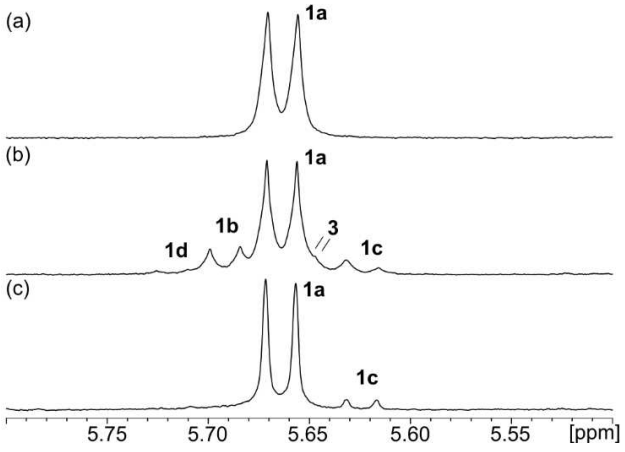

Figure 2. H5 doublets of 1 MeU ligands of **1 a**: (a) immediately after dissolving in D_2O (0.02 M, ambient temperature; 500 MHz); (b) after 6 weeks at room temperature; (c) 20 months after addition of solid NaCl (0.13 M).

next to that of the major signal **1 a**. Regarding the assignments of the other signals, we consider hydrolysis species, condensation products, as well as species short of an ammonia ligand as being responsible for their appearance (Scheme 2).

*Hydrolysis product of **1 a**:* The H5 signal closest downfield to **1 a** is readily assigned to its hydrolysis product, *cis*-$[Pt(NH_3)_2(1MeU\text{-}N3)(OD_2)]^+$ (**1 b**), in fast equilibrium with **1 b'**, as it is formed by abstracting Cl^- from **1 a** with $AgNO_3$ (see below). The pK_a of **1 b** is ca. 7.[13]

*Condensation reactions involving **1 a** and **1 b**:* Scheme 3 lists potential dinuclear condensation products derived from **1 b** (self-condensation) or from **1 a** and **1 b** (co-condensation), which represent the two main species present in solution. Only two of these contain exclusively terminal 1MeU ligands and are therefore relevant in the context of the solution behavior of **1 a**. As indicated in Scheme 3, condensation reactions can take place in different ways, leading altogether to five different products, (A)–(E). We assign the H5 signal at 5.64 ppm to the μ-hydroxido species *cis*-$[(NH_3)_2(1MeU)Pt(\mu\text{-}OH)Pt(1MeU)(NH_3)_2]^+$(**3**), which corresponds to product (A) in Scheme 3, based on its chemical shifts.[4,13] Much to our surprise, ^1H NMR signals of the well-known *head-tail* dinuclear complex *cis*-$[Pt_2(NH_3)_4(1MeU\text{-}N3,O4)_2]^{2+}$ (**4**)[16], hence condensation product (C) in Scheme 3, are absent in this spectrum. We attribute this fact to the neutral to slightly alkaline pD of the sample (see below), which obviously favors μ-OH bridging over μ-1MeU bridging. It is noted, that in the (en)Pd^{II}/uridine system likewise no *head-tail* dimer is formed in moderately alkaline solution (pH 9).[17] With solutions containing **1 b** in higher concentrations, larger condensation products may form, as outlined for the simplest case of self-condensation of *three* **1 b** units in Figure S3. Both linear bis(μ-1MeU), mixed μ-OH, μ-1MeU, as well as a cyclic trinuclear species are feasible. There is X-ray structural evidence for the existence of cyclic trinuclear complexes of Pt^{II}[18] as well as Pd^{II}[19] with closely related 1-methylcytosine nucleobases which bridge in a N3,N4 fashion. In principle some of the linear Pt_3 compounds could form larger oligomers as also indicated in Figure S3. If, in addition also condensation reactions involving the other mononuclear species given in Scheme 2 are considered, the number of possible products increases dramatically. A further complication, namely the possibility of condensation reactions between Pt–OH and H_3N–Pt units, leading to μ-NH_2 species, is not even discussed here (see, however, below) even though there is evidence that such reactions can take place in water.[20,21]

*Release of NH_3 from **1 a**.* In Scheme 2 (right side) we have also taken into account the possibility that a NH_3 ligand is removed from **1 a** as a consequence of the kinetic *trans*-effect of the chloride ligand to produce **1 c** and its hydrolysis products, respectively. In general, and in particular for preparative purposes, a large excess of chloride (HCl, NEt_4Cl) and forcing conditions (elevated temperature) are necessary to convert, for example, *cis*-$[Pt(NH_3)_2Cl_2]$ completely into $[Pt(NH_3)Cl_3]^-$,[22] but there are also cases of NH_3 release under mild conditions,[23] albeit in low yield. The latter situation, possibly also relevant to **1 a** here, might be rationalized by an interaction of neutral **1 a**

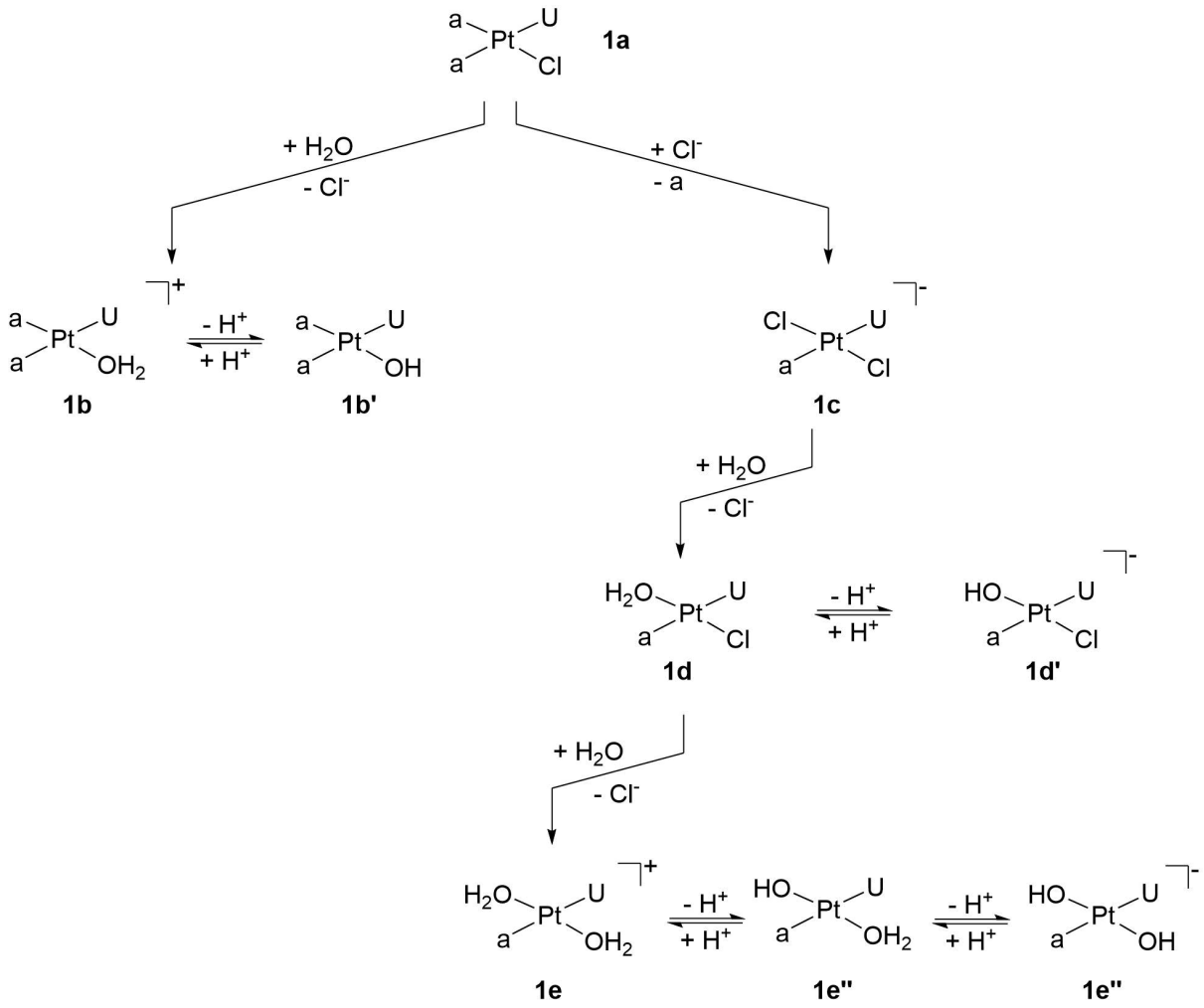

Scheme 2. Hydrolysis products of **1 a** (left) and hydrolysis products of **1 c** (right). U = 1-methyluracil anion (1MeU-*N3*); a = NH_3

with chloride ions originating from partial hydrolysis of the very same species **1 a** (Scheme 4).

In order to further verify such a possibility, we have added solid NaCl to the solution and allowed it to age (Figure 2 (c)). Under these conditions the H5 doublet at 5.62 ppm increases in intensity at the expense of the other minor ones, eventually reaching approximately 10% of the intensity of **1 a**. In a parallel experiment, carried out in water under identical conditions of **1 a** and NaCl, it was found that the pH of the solution changes from 5.5 after the first day to 6.8 within two weeks at room temperature, suggesting formation of ammonia. We cannot exclude the possibility that released NH_3 interacts with **1 b** to form $[Pt(NH_3)_3(1MeU\text{-}N3)]^+$, as chemical shifts of such a species are virtually identical with those of **1 b**. However, the observed rise in pH seems not to be consistent with such a reaction playing a major role. As to the remaining H5 signal furthest downfield (5.72 ppm), its chemical shift is still close to species with terminal 1MeU-*N3* ligands rather than bridging ones, and therefore it is tentatively assigned to one of the hydrolysis products of **1 c**, possibly **1 d**.

2.3. ESI-Mass Spectra of 1 a

Electro Spray Ionization (ESI) mass spectra of aqueous solutions of **1 a** were recorded. Figure 3 provides a typical overview. As can be seen, major peaks are clustered around *m/z* 400, 800, 1200, 1400, and 1600. These species are attributed to ions of Pt(1MeU), $Pt_2(1MeU)_2$, $Pt_3(1MeU)_3$, $Pt_4(1MeU)_3$, and $Pt_4(1MeU)_4$ stoichiometries, based on rough calculations regarding the

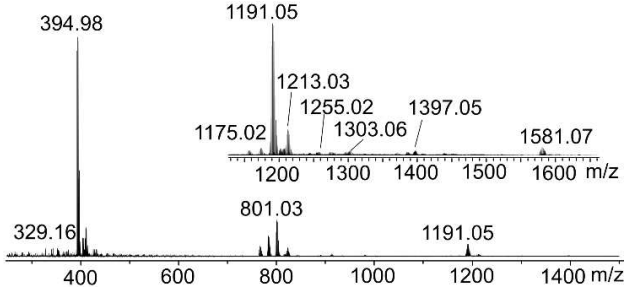

Figure 3. ESI-mass spectrum of **1 a**, dissolved in water (1 mg in 1 mL).

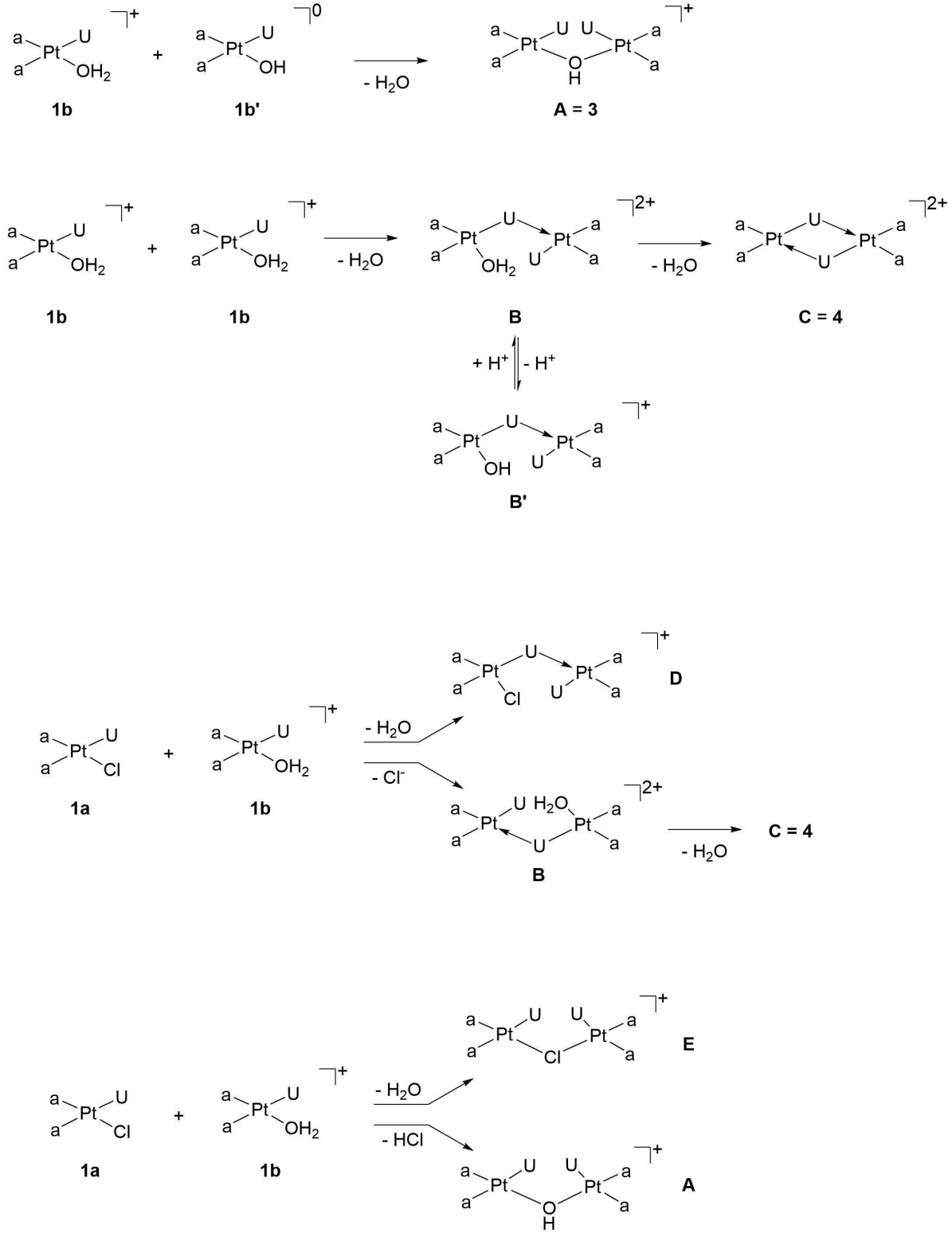

Scheme 3. Possible dinuclear products formed upon self-condensation of **1 b** or co-condensation between **1 a** and **1 b**. U = 1-methyluracil anion (1MeU-*N3*); -U- > = μ-1MeU-*N3*,*O4*; a = NH_3. Note that **A** and **B'** are geometrical isomers, as are **D** and **E**. Feasible alternative condensation products derived from other, minor Pt species (as listed in Scheme 2) are not considered. For possible μ-NH_2 condensation products see Scheme 5.

masses of Pt and 1MeU units, plus co-ligands and possible counter-ions (Na^+ and Cl^-) to give +1 cations. Most of the signals indeed reveal spacings of one nominal mass between the lines of the isotopic patterns, thus confirming +1 charges of these cations.

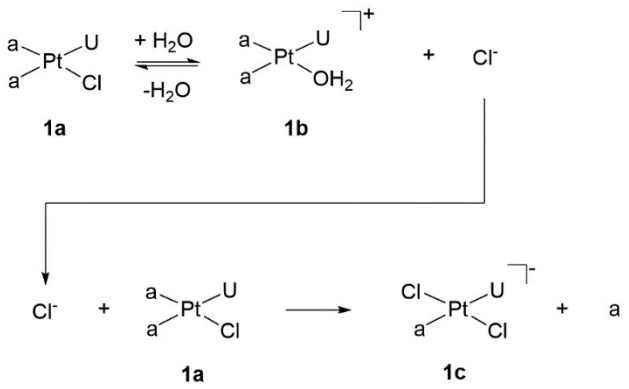

Scheme 4. Feasible pathway from **1 a** to **1 c**, taking advantage of chloride ions released during hydrolysis of **1 a**. U = 1 MeU-*N3*; a = NH_3.

The most intense signal is that of *m/z* 395. In agreement with simulations, it is attributed to composition {Na[Pt(NH_3)(1MeU)Cl]}$^+$ (Figure 4). Obviously, one of the original ammonia ligands of **1 a** has been lost, supporting our solution findings. It should be pointed out that numerous scenarios exist as to how NH_3 may be liberated,[24] and that in particular in MS experiments with biomolecules and Cisplatin, release of NH_3 is a common phenomenon.[25] The ion detected with *m/z* 395 is either a three-coordinate Pt^{II} complex, or a four-coordinate compound with 1MeU chelating the metal via N3 and one of its two exocyclic O4 or O2 oxygen atoms. In general, N,O chelation of pyrimidine nucleobases is not observed in solid state structures of Pt^{II} complexes as a consequence of unfavorable bonding angles within such a chelate, but there are (rare) cases of N,O chelates for Pd^{II},[26] or – less uncommon – for octahedral metal ions, e.g., Cp*Rh^{III}.[27]

The weak signal at *m/z* 412 is assigned to the Na^+ adduct of **1 a**, hence to {Na[Pt(NH_3)$_2$(1MeU)Cl]}$^+$ (not shown). Also, an ion resulting from a loss of chloride, hence [Pt(NH_3)$_2$(1MeU)]$^+$ (with *m/z* 354), is observed, yet not pointing to the presence of any

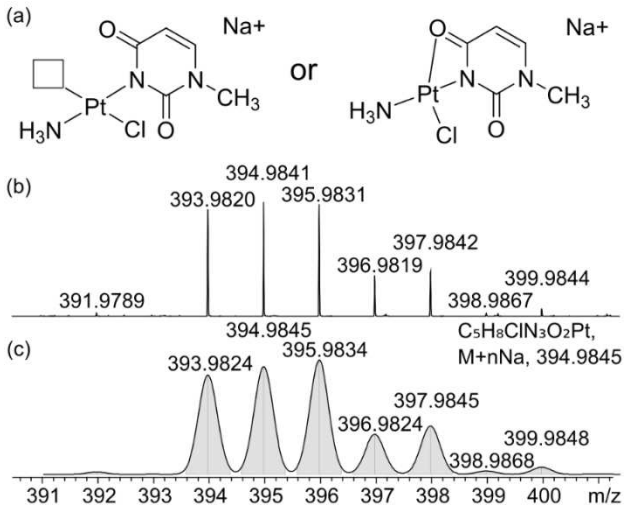

Figure 4. (a) Derivative of **1 a** following loss of one of the NH_3 ligands. (b) Experimental ESI-mass spectrum. (c) Simulation.

of the other species detected following reaction of **1 a** with $AgNO_3$ (see below).

A more detailed analysis of the spectrum reveals certain "series" of signals. For example, the signals at *m/z* 395 and 767 fit compositions of {Na[Pt(NH_3)(1MeU)Cl]$_n$}$^+$ with n = 1 and 2, respectively, and the signals at *m/z* 412, 801, 1191, and 1581 fit {Na[Pt(NH_3)$_2$(1MeU)Cl]$_n$}$^+$ with n = 1, 2, 3, and 4. It appears that the *m/z* 1581 signal superimposes a second weak signal of a +2 charged species (spacing 0.5 mass units), which is attributed to a dimer, {Na$_2$[Pt(NH_3)$_2$(1MeU)Cl]$_8$}$^{2+}$. There is a third mini-series consisting of species assigned to {Na[Pt(NH_3)$_2$(1MeU)Cl]$_n$ [Pt(NH_3)(1MeU)Cl]}$^+$, hence a mixture of the two basic entities **1 a** and the one that has lost an ammonia ligand: n = 1 gives *m/z* 784, and n = 2 leads to *m/z* 1175. Finally, there are numerous weak and in part overlapping sets of signals in the *m/z* range 1250–1500 which are due to +2 cations, as evident from their spacing patterns. Masses of these entities are thus between 2500 and 3000, suggesting aggregates containing between 6 and 8 Pt complexes. One of these, centered at *m/z* 1386, could be be due to a species of composition {Na$_2$[Pt(NH_3)$_2$(1MeU)Cl]$_7$}$^{2+}$. Additional ESI-MS experiments, in which **1 a** had been mixed with NaX salts (X = NO_3^-, Cl^-) in 2:1-ratios, had provided rather similar results, thus supporting the above interpretation.

Regarding possible structures of the various cations, these can be ambiguous. For example, for *m/z* 767 both a stacked arrangement of two neutral [Pt(NH_3)(1MeU)Cl] units cross-linked by a Na^+, or a dinuclear *head-tail* species of composition {Na[(NH_3)ClPt(μ-1MeU)$_2$PtCl(NH_3)]}$^+$ are feasible. Clearly, the interchange between these two options is a very minor one, a change from chelation of 1MeU to a bridging mode. A third possibility would be a dinuclear species with a single chloride bridge (Figure S4). Simulation cannot differentiate between these possibilities. The simplest interpretation of the *m/z* 784 peak would be a loose association between {Na[Pt(NH_3)$_2$(1MeU)Cl]}$^+$ and [Pt(NH_3)(1MeU)Cl]. Alternatively, dinuclear species with a single 1MeU bridge and a terminal 1MeU ligand, {Na[(NH_3)$_2$Cl(μ-1MeU)Pt(NH_3)Cl(1MeU)]}$^+$, or with a single Cl^- bridge and two terminal 1MeU ligands would likewise be consistent with the mass observed. The series fitting {Na[Pt(NH_3)$_2$(1MeU)Cl]$_n$}$^+$ with n = 1, 2, 3, and 4 does not allow for any structures containing μ-1MeU or μ-Cl ligands. There exists, however, still the possibility that the Na^+ ion becomes bonded to Cl ligands and/or exocyclic O sites of 1MeU ligands.[28] In a way, the occurrence of a series of Na^+ adducts is reminiscent of the so-called "magic number clusters" of unsubstituted uracil in the presence of alkali metal ions, including those of Na^+.[29] The flat uracil quartet having a single sodium ion in its center, is particularly stable and has been observed also in the solid and on Au(111) surfaces.[30] The structure of an analogous {Na[**1 a**]$_4$}$^+$ with n = 4 (*m/z* 1581) would need to be fundamentally different from the classical uracil quartet, however, since the proton at N3 is no longer available for hydrogen bonding with an adjacent O4. In principle, rotation of the four uracil rings about their O4-C4 bonds would avoid steric clash between the Pt entities and moreover might allow for some weak hydrogen bonds between the aromatic protons at C5 and O4 sites (Figure 5). Such unconventional C-H···O contacts are occasion-

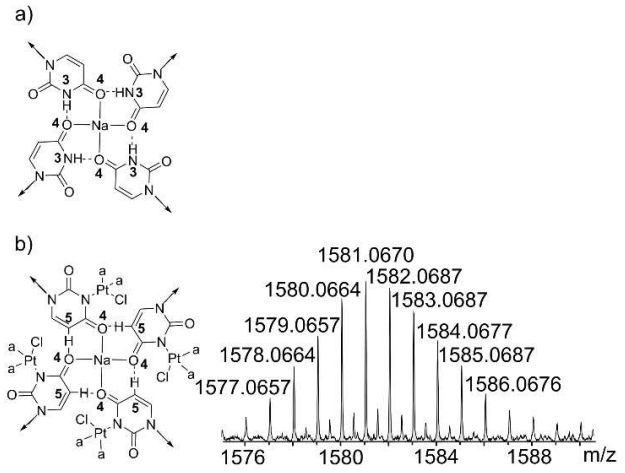

Figure 5. Classical Na[1MeUH]$_4$-quartet (a). Feasible, simplified structure derived from **1 a**, $\{Na[PtUa_2Cl]_4\}^+$, and its ESI-MS signal (m/z = 1581) (b). Minor set presumably is due to dimer $\{Na_2[PtUa_2Cl]_8\}^{2+}$.

ally observed with uracil nucleobases[31] and have been the subject of theoretical work.[32] DFT calculations are planned to further study this aspect.

In our analysis of the mass spectra data we have also considered the option that neutral NH_3 ligands are partially substituted by OH^-, since both ligands have nearly identical masses. This change does, however, require alterations in Pt oxidation states. In all cases discussed above, the Pt ions have retained their +II oxidation states. When considering mixed-valence $Pt^{II}Pt^{III}$or $[Pt^{III}]_2$ species instead (with appropriate replacement of NH_3 and an increase in Pt coordination numbers), simulations give stunningly similar spectra, but a closer look at the mass accuracy data (in the order of 1 ppm for Pt^{II},Pt^{II} ; in the order of 30 ppm for Pt^{II},Pt^{III} and Pt^{III},Pt^{III}) favors an interpretation of the observed signal sets as being due to dinuclear Pt^{II} complexes. This view gets further support by the signals centered at *m/z* 1191 and 1581, which agree excellently with simulations for $\{Na[Pt(NH_3)_2(1MeU)Cl]_3\}^+$ and $\{Na[Pt(NH_3)_2(1MeU)Cl]_4\}^+$, respectively (see above), yet not nearly as well with those of tri- and tetranuclear Pt species containing different combinations of Pt^{II}, Pt^{III}, and Pt^{IV} as well as OH^- and NH_2^- instead of NH_3 to account for proper +1 charges.

2.4. Solution Behavior of *cis*-[Pt(NH$_3$)$_2$(1MeU-*N3*)Cl]·H$_2$O (1 a) in Presence of AgNO$_3$

When $AgNO_3$ is added to a suspension of **1 a** in H_2O or D_2O, e.g. 1 equiv., **1 a** becomes immediately dissolved, leading to an essentially transparent solution. Precipitation of AgCl starts only gradually. This behavior suggests initial formation of a cationic, water-soluble heteronuclear Pt,Ag_x complex (x = presumably 1 or 0.5). Ag^+ could be coordinated to an exocyclic oxygen atom of 1MeU, to the chloride ligand, directly to Pt^{II}, or a combination of these. There is evidence for all such possibilities.[33,34] AgCl filtration after 24 h yields a colorless, moderately acidic solution ([Pt] typically 0.02 M; pH 3–3.4). As previously described by us,[13] subsequent cooling gives colorless microneedles of *cis*-[Pt(NH$_3$)$_2$(1MeU-*N3*)(OH$_2$)]NO$_3$ (**1 b**) as a first fraction, and upon slow, partial evaporation, greenish-yellow crystals of the *head-tail* dinuclear compound *cis*-[Pt$_2$(NH$_3$)$_4$(1MeU-*N3,O4*)$_2$](NO$_3$)$_2$·3H$_2$O (**4**). At this point, the solution has turned blue. Other products were neither isolated nor characterized.

When varying reaction conditions of the above reaction (**1 a** + $AgNO_3$) and in particular the workup, it soon became evident that the "history of sample handling" had a major effect on the composition of the reaction mixture. Specifically, it made a substantial difference whether or not the sample studied had been brought to dryness prior to studying its ^{1}H NMR spectra, and how the process of solvent removal had been achieved, by slow evaporation in air or by evaporation with a vacuum pump. Sample concentration likewise had a major effect on species distribution. Among others, **1 a** and $AgNO_3$ were mixed in different ratios, namely 1:1.2, 1:1, and 1:0.8, allowed to react for different lengths of time (24 h vs. 4 days, room temperature, daylight excluded), and were either directly studied in solution (D_2O), or following solvent removal and subsequent re-dissolving the solid in water (D_2O for NMR or H_2O for ESI-MS). We were particularly interested in finding out whether Ag^+ was functioning exclusively as a chloride-abstracting reagent in the above reaction, or if it was possibly also acting as an oxidant. After all, oxidative ligand dimerization[35] and metal oxidation[36] have been observed with Pt^{II} complexes when reacted with silver salts. We even considered the possibility that part of the added Ag^+ could be complexed by NH_3 released from **1 a**.[37]

In the following, selected examples will be discussed in more detail, divided in three sections with (I) an excess of $AgNO_3$ applied over **1 a**, with (II) a substoichiometric amount of $AgNO_3$ applied, and (III) with **1 a** and $AgNO_3$ reacted in a 1:1-ratio. Before doing so, let us briefly return to some general aspects concerning condensation reactions involving **1 b** and **1b'**. Both compounds have three ligands capable of undergoing such reactions: H_2O/OH^-, $1MeU^-$, and NH_3. There is ample structural evidence for the existence of μ-OH, μ-1MeU, and μ-NH_2 bridges in Pt^{II} coordination chemistry.[4,20,38] Scheme 5 summarizes the various possibilities relevant to **1 b** and **1b'**. As to the μ-amido species, the non-equivalence of the two NH_3 ligands in **1 b** and **1b'** leads to four possible products, which are pairwise geometrical isomers (**F**, **G**; **F'**, **G'**) and at the same time are pairwise involved in acid-base equilibria (**F**, **F'**; **G**, **G'**). In addition, a bis(μ-NH_2) product **H** and a mixed μ-NH_2, μ-1MeU product **I** are feasible. Moreover, the compounds with single bridges could occur as different rotamers, which in the NMR spectra would further complicate their appearance. In summary, different condensation modes, different diastereomers *and* different rotamers could explain the complexity of even the simplest, dinuclear condensation products of **1 b**.

*Slight excess of AgNO$_3$ (1.1–1.2 equiv.) over **1 a*** (I): The first ^{1}H NMR spectrum, recorded 24 h after start, reveals the presence of the majority species *cis*-[Pt(NH$_3$)$_2$(1MeU-*N3*)(OD$_2$)]$^+$ (**1 b**) as well as of three species of moderate intensities, namely unreacted $\{1a{\cdot}Ag_x\}^{x+}$, the μ-OD species **3**, and the *head-tail* dimer **4**. As compared to **1 a**, all 1MeU resonances are slightly downfield shifted in the Ag^+ adduct. Within several days, **4**

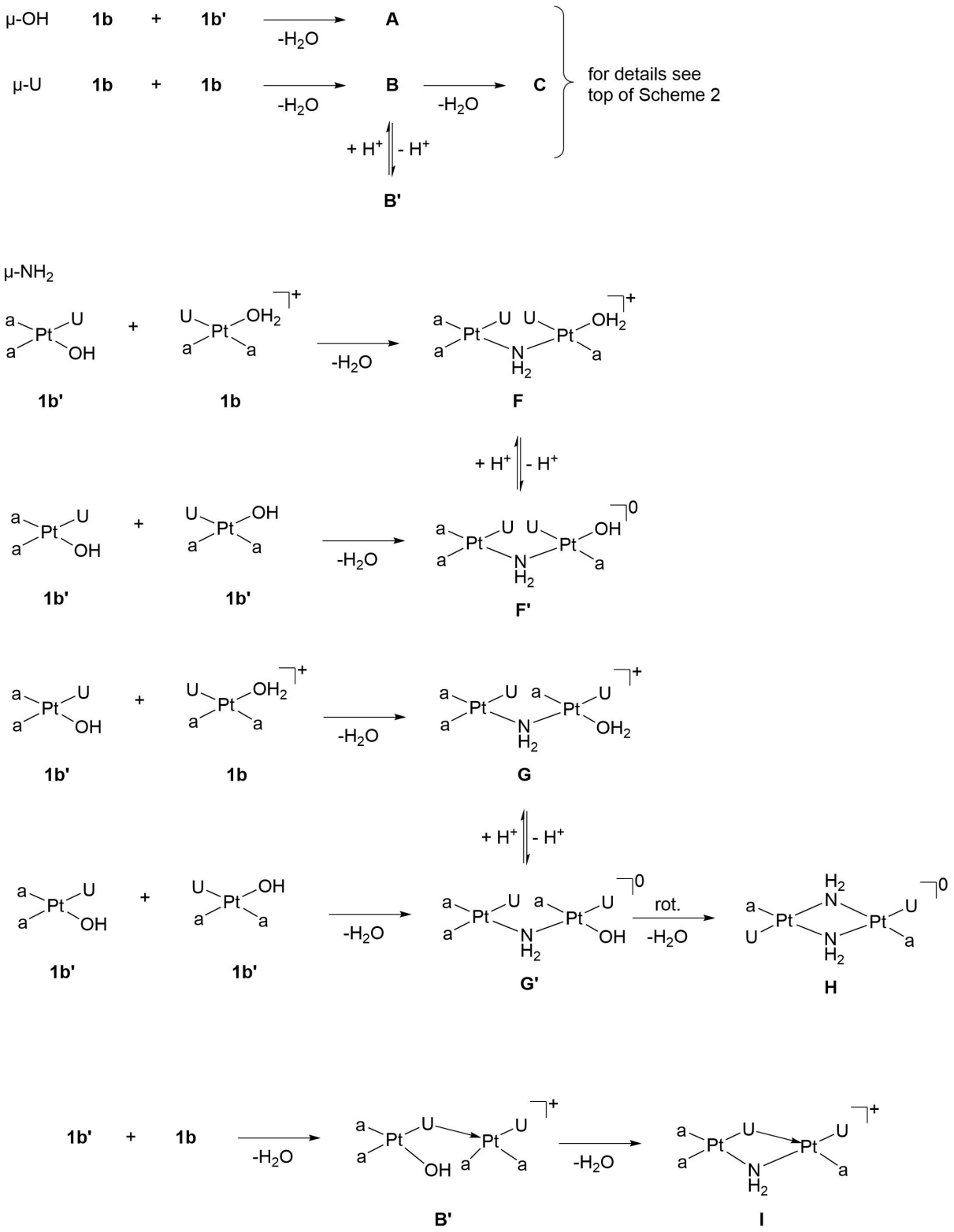

Scheme 5. Dinuclear condensation products, including μ-NH_2 species, derived from **1 b**/**1 b′**. Among the μ-NH_2 complexes, **F**, **G** and **F′**, **G′**, respectively, are geometrical isomers.

surpasses **3** in intensity, but **1 b** remains the dominant species. After 3 weeks, relative signal intensities of **1 b**, **4**, and **3** are 64:26:8, corresponding to a mole ratio of 64:13:4. Expectedly, signals due to $\{\mathbf{1a}_n\mathbf{Ag}_x\}^{x+}$ have disappeared by then (Figure S5). The three mentioned compounds thus account for 98% of total 1MeU resonances. As to the remaining 2%, they are attributed to minor components (see below).

Sample brought to dryness prior to NMR study. In a parallel experiment, carried out in H_2O for 4 days under otherwise identical conditions, the solution obtained after AgCl filtration was allowed to slowly evaporate to dryness over a period of several days. By then the resulting solid had adopted a dark blue color and its UV-vis spectrum exhibited a broad absorption band at 649 nm. The ^{1}H NMR spectrum of this sample displayed at least six sets of 1MeU resonances (Figure 6 (a)), with the three major ones (**4**, **3**, **1 b**) accounting for some 82% of total signal intensity.

Within 3 weeks (sample kept in dark at room temperature) the spectrum undergoes dramatic changes (Figure 6 (b)), with **1 b** becoming the dominant species (60.1% of total intensity), followed by **3** (22.4%) and **4** (7.4%). Three minor sets of resonances add up to ca. 10%.

Quite obviously, the equilibrium 2 (**1 b**) = **4** + $2H_2O$ is concentration-dependent: Once formed in concentrated solution (during sample evaporation) the *head-tail* dimer **4** slowly dissociates again to the monomer **1 b**, when redissolved, and in particular in more dilute solution.

Regarding the minor components seen in the ^{1}H NMR spectra: The excess of Ag^+ ions applied in this experiment eventually ends up in the heteronuclear complex *cis*-{[Pt$(NH_3)_2$(1MeU-*N3*)$_2$ $Ag_x]^{x+}$ (**2 a**), with its H5 doublet furthest upfield. Resonances of **2** are at 7.30 (H6), 5.53 (H5), and 3.27 (CH_3) ppm, but Ag^+ coordination causes downfield shifts in **2 a**, very much as in the case of the Ag^+ adduct of **1 a**. An example of Pt_2Ag stoichiometry has previously been reported by us for the 1-methylthymine analogue.[34a] What strikes is the fact that in this sample (and practically in all other samples studied, also with no excess of $AgNO_3$; for details see (II)), over time the amount of **2** increases substantially in comparison to the amount of impurity seen in **1 a** (see above). Two scenarios may be considered to explain this finding: (i) A partial isomerization of the *head-tail* dimer **4** into the corresponding *head-head* dimer **5**, followed by a partial dissociation of **5** into **2** and the diaqua species *cis*-[Pt$(NH_3)_2(OD_2)_2]^{2+}$. Similar isomerization processes have been reported before for a dinuclear Pt^{II} complex containing cyclic amide bridges.[39] Indeed, one of the minor H5 doublets, the one closest to H5 of **4**, could possibly be due to the *head-head* dimer **5** (Figure 6). (ii) A second option might be that **2** is formed in a disproportionation reaction according to (**1 b**) = 0.5 (**2**) + 0.5 (*cis*-[Pt$(NH_3)_2(OD_2)_2]^{2+}$), which likewise could explain subsequent formation of **5**. Regardless of the mechanism leading to an increase in **2** it is clear that such a process is accompanied by formation of diaqua species. This fact may be relevant to rationalize formation of aggregates of Pt_2U or Pt_3U_2 stoichiometries, for example.

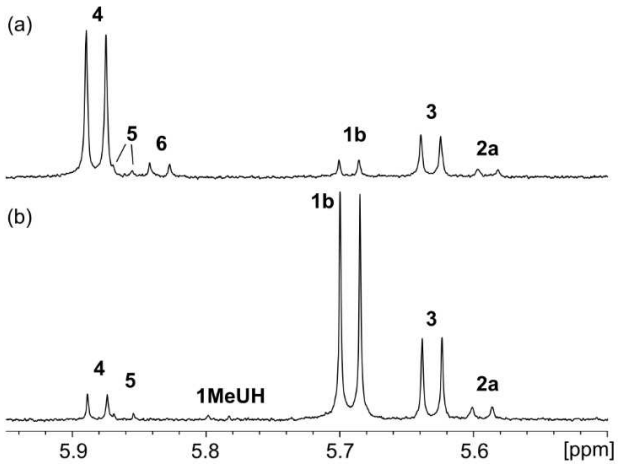

Figure 6. H5 resonances of 1MeU ligands of products present in a sample of **1 a** reacted with 1.2 equiv. of $AgNO_3$ (4 days), centrifuged from AgCl, evaporated to dryness, and re-dissolved in D_2O: (a) immediately after dissolving; (b) 3 weeks later.

As to the H5 doublet at 5.835 ppm, seen in the spectrum immediately after dissolving the evaporated sample in D_2O (Figure 6 (a)), it is close to resonances of μ-1MeU species (**4** and possibly **5**) rather than to terminal (1MeU-*N3*) ligands, which are upfield by some 0.15–0.25 ppm. Its H6 counterpart at 7.38 ppm (established by ^{1}H,^{1}H-COSY[4]) is likewise close to H6 of **4**, which is at 7.40 ppm. We propose that these signals correspond to a trinuclear complex (**6**), as it is only seen in concentrated solutions and, according to a DOSY spectrum (DOSY = *D*iffusion *O*rdered *S*pectroscop*Y*), is larger than the *head-tail* dimer **4**. As mentioned already, there is crystallographic evidence for the existence of both *head-tail* dimers *and* cyclic trimers in the related 1-methylcytosine system with Pt^{II} and Pd^{II}[18,19,40], and within supramolecular chemistry equilibria between di-and trinuclear or higher nuclearity species in dependence of concentration and temperature are well established.[41] Nevertheless we do not believe that **6** is a cyclic trimer, *cis*-{[Pt$(NH_3)_2$(1MeU-*N3,O4*)$_3]_3\}^{3+}$, simply because the H5 resonance of a bridging 1MeU within such a cycle should resonate at substantially lower field than observed, as a consequence of Pt pointing toward H5. We are aware that an assignment to a linear trinuclear compound formed from three entities of **1 a** (see Figure S3) requires the presence of an additional terminal 1MeU ligand, which might be buried beneath the other sets, however. An alternative linear structure, in which a terminal 1MeU has been lost, hence giving a Pt_3(μ-1MeU)$_2$ stoichiometry would solve this dilemma.

Sub-stoichiometric amounts of $AgNO_3$ (II): **1 a** was also reacted with 0.8 equiv. of $AgNO_3$ for four days and, following removal of AgCl, the solution was allowed to evaporate to dryness. The obtained dark blue product displays two broad absorptions at 560 and 684 nm in the UV-vis spectrum. The ^{1}H NMR spectrum (D_2O) is similar to that discussed above with excess of $AgNO_3$ with **4** being the dominant species (Figure S6 (a)), followed by **3**, unreacted **1 a**, **1 b**, **6**, **2**, and **5**. Ageing of this solution for three weeks again causes a reversal in abundance of **4** and **1 b** (Figure S6 (b)). The 1MeU signal intensity of *cis*-[Pt$(NH_3)_2$(1MeU-*N3*)$_2$] (**2**) amounts to 10%, corresponding to a 5% abundance of this compound, and hence a 40-fold increase compared to its presence as an impurity in **1 a**. Compound **6** is no longer present.

***1 a** and $AgNO_3$ in 1:1-ratio* (III): The filtrate obtained after a reaction time of 24 h and removal of AgCl was vacuum-evaporated during a period of 48 h, and analyzed by elemental analysis, EDX (*E*nergy*D*ispersive*X*-ray spectroscopy)), IR spectroscopy, and ^{1}H NMR. The IR spectrum of the colorless material

obtained was identical with that of the previously characterized $[Pt(NH_3)_2(1MeU)(OH_2)]NO_3$,[13] as were elemental analysis data. However, EDX revealed the presence of residual Ag^+ and Cl^-. Rather than originating from admixed AgCl, it is believed that it is largely due to $\{\mathbf{1a}\cdot\mathbf{Ag}_x\}^{x+}$, as suggested by the ^{1}H NMR spectra (see below). The ^{1}H NMR spectra of this material, recorded at two different concentrations (0.02 M and 0.1 M), proved the most complicated ones (Figure 7), both with respect to the multitude of signals and their time- and concentration dependence. Immediately after sample preparation the by far dominating species is the monomer **1b**, regardless of concentration. A small amount of unreacted **1a**, present as its Ag adduct $\{\mathbf{1a}\cdot\mathbf{Ag}_x\}^{x+}$ and recognized by its downfield shift, is identified. Both **3** and **4** represent minor species at this stage. There is also an as yet unidentified species "**X**" present, to be briefly discussed below, together with other species observed at a later stage. Within two days, during which the solution adopts a blue-purple color, signals of the *head-tail* dimer **4** strongly increase in intensity and a series of new resonances appear. Within two weeks, signals of **4** have surpassed those of **1b** in intensity in the more concentrated solution (0.1 M), and the intensity of signals of the μ-OH dimer **3** is about one third of **4**. It strikes that even after 11 weeks signals of **1a** (no longer downfield shifted) are still clearly discernible, regardless of concentration. This observation corroborates our suspicion that Ag^+ not only acts as a chloride abstractor on **1a**.

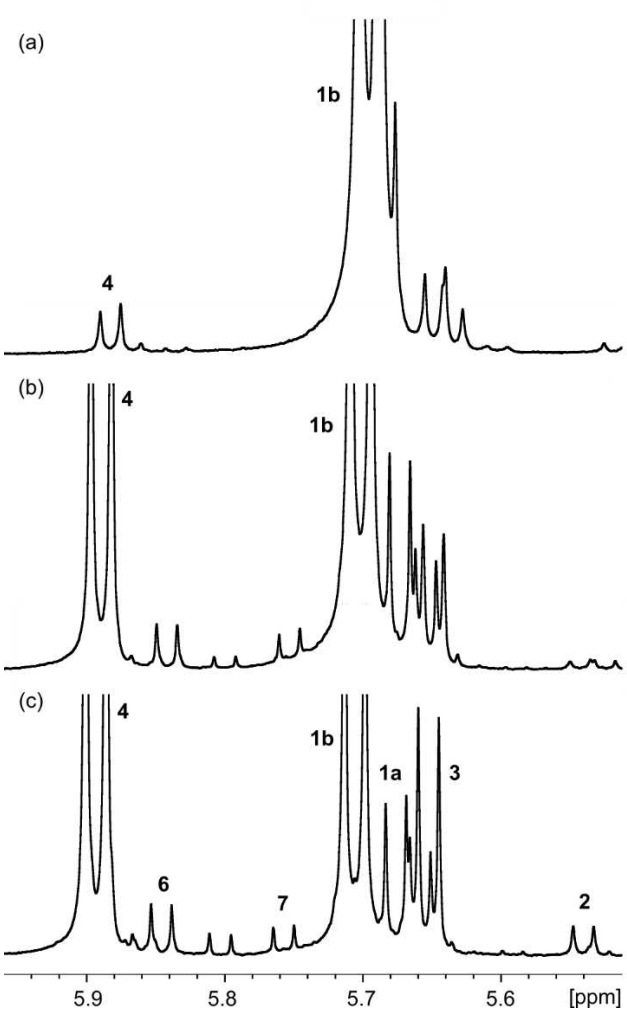

Figure 7. H5 resonances of 1MeU ligands of species derived from rotary evaporated **1b**, re-dissolved in D_2O (0.1 M, ambient temperature): (a) Immediately after sample preparation; (b) two days later (sample is blue-purple); (c) two weeks later. The doublet next to **3** and that between the doublets of **6** and **7** are presently unidentified, as are additional doublets of very low intensities or partially overlapping with other signals.

A comparison of spectra recorded with different concentrations reveals some interesting differences: For example, in the dilute sample (0.02 M) relative intensities of the three major species are **1b** > **3** > **4**, unlike in the concentrated solution discussed in the previous paragraph. In the dilute sample the species with its H5 doublet at 5.74 ppm (and its H6 at 7.50 ppm) (**7**) is more intense than the H5 doublet at 5.84 ppm, which tentatively has been assigned to trimer **6**, whereas the situation is reversed in the concentrated solution. According to DOSY experiments the two species differ in size: While, as mentioned above, **6** is larger than dinuclear **3**, the size of **7** is close to that of the monomer **1b**. The H5 chemical shift of **7** is indeed near that of the species in Figure 2, which had been tentatively attributed to a monomeric hydrolysis product of **1c** (see above). Needless to say, that signals due to **2** have increased here too.

During long reaction times (2.5 months) additional changes take place in the spectra, such as the appearance of a "bump" of H6 resonances beyond 7 ppm, similar to the situation with "Pt pyrimidine blues",[4] and resonances near 6.5 ppm (Figure S7). We are presently unable to assign these signals.

Let us briefly return to signals "**X**", present in ca. 4% abundance from the beginning, and not changing with time. Its ^{1}H NMR resonances occur at 3.90 (s, CH_3), 7.00 (H5) and 8.43 ppm (H6), and are quite substantially remote from signals of any of the other species discussed. Moreover, they display fine structures of the H6 and H5 resonances not seen with any of the other signals (Figure S7). A homo-decoupling experiment reveals that the splitting patterns are due to superimposed doublets and hence originate from pure proton-proton coupling. We have to admit that despite several attempts, we have been unable to reproduce formation of this species. All we can be sure of is that it is a kinetically robust species, and that according to DOSY, the size of "**X**" is in between that of monomeric **1b** and dinuclear **4** (Figure S8). See also section below.

2.5. ESI-Mass Spectra of 1a Treated with $AgNO_3$

Solids obtained by reacting **1a** with $AgNO_3$ in the ways described above (I–III) were subjected to ESI-mass spectrometry after being redissolved in water. With few exceptions, to be detailed below, the spectra obtained are rather similar, with relative intensities of signals occasionally inverted, however. In general, +1 cations are detected, and only occasionally +2 cations. The isotopic distribution patterns of individual signals proved to be helpful in the assignments. Thus, mononuclear Pt compounds usually give rise to five clearly discernible lines,

while 7–9 lines are differentiated for Pt_2 compounds, 11–13 lines for Pt_3 species, and 15 −18 lines for Pt_4 compounds. Additional isotopomers are of very low abundance and difficult to identify. While not unexpected for sample (II), chloride containing species are also observed for (III), and weakly even for (I). The presence of Ag, expected in the mass spectrum of sample (I), is also detected in (III). The most significant finding, in particular with compounds containing two or more Pt centers, is *the co-existence of species with closely similar masses.* This appears to be a consequence of the similarity in masses of NH_3 and OH^-, of NH_2^- and O^{2-}, or of Cl^- and (NH_3+OH_2). Their presence points to different ways of formation and may be a clue to understand the complexity of composition of species formed during condensation reactions of the seemingly simple monomeric *cis*-$[Pt(NH_3)_2(1MeU)(OH_2)]^+$. Simulations were applied to differentiate the various options and the mass accuracy was used as a criterion for the most likely composition of a particular species.

In the following, we concentrate on the most prominent signals only and shall discuss selected examples. Figure 8 provides an overview of the ESI-mass spectrum of sample (III), hence the solid obtained by treating **1 a** with $AgNO_3$ in a 1:1-ratio following a workup as mentioned above. Overviews of the mass spectra of the two other samples are given in the Supporting Information (Figure S9).

In all three cases the most intense peaks are below *m/z* 400, with *m/z* 354 representing the major one. It is attributed to $[Pt^{II}(NH_3)_2(1MeU)]^+$ (Figure 9). The second most intense peak is centered at *m/z* 365, followed by the signal at *m/z* 348. These two sets of signals are assigned to $[Pt^{II}(NH_3)(1MeU)(N_2)]^+$ and $[Pt^{II}(1MeU)(N_2)]^+$, respectively. They were fully unexpected, and we shall discuss them separately (see below). Two more signals, partly overlapping and of approximately equal and moderate intensities, are assigned to $[Pt^{II}(NH_3)(1MeU)]^+$ (*m/z* 337) and to $[Pt^{II}(1MeU)(OH_2)]^+$ (*m/z* 338).

Another intense signal, centered at *m/z* 446, and present *only* in sample (III) is tentatively assigned to species **"X"** seen *only* in the ^1H NMR spectrum of (III). Its isotopic distribution pattern (Figure S10) clearly identifies it as a mononuclear Pt complex, consistent with the results of the DOSY solution spectrum (see above). We tentatively assign this species to a Pt^{IV} complex based on its unusually downfield shifted proton resonances and its apparent inertness. Simulations were carried out for a series of possible compositions, but none gave a fully convincing result.[42]

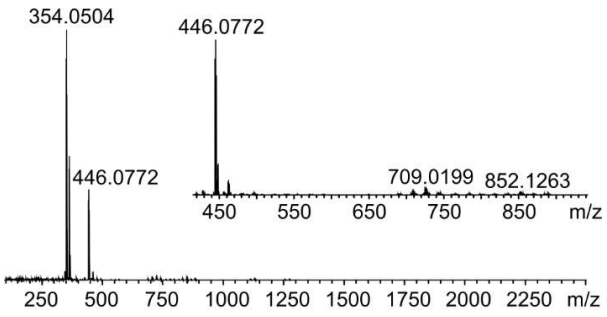

Figure 8. ESI-MS spectrum of sample (III), prepared from **1 a** + $AgNO_3$ (1:1, 4d, 22 °C, in dark), centrifugation of AgCl, evaporation to dryness, and dissolving in H_2O (1 mg in 1 mL).

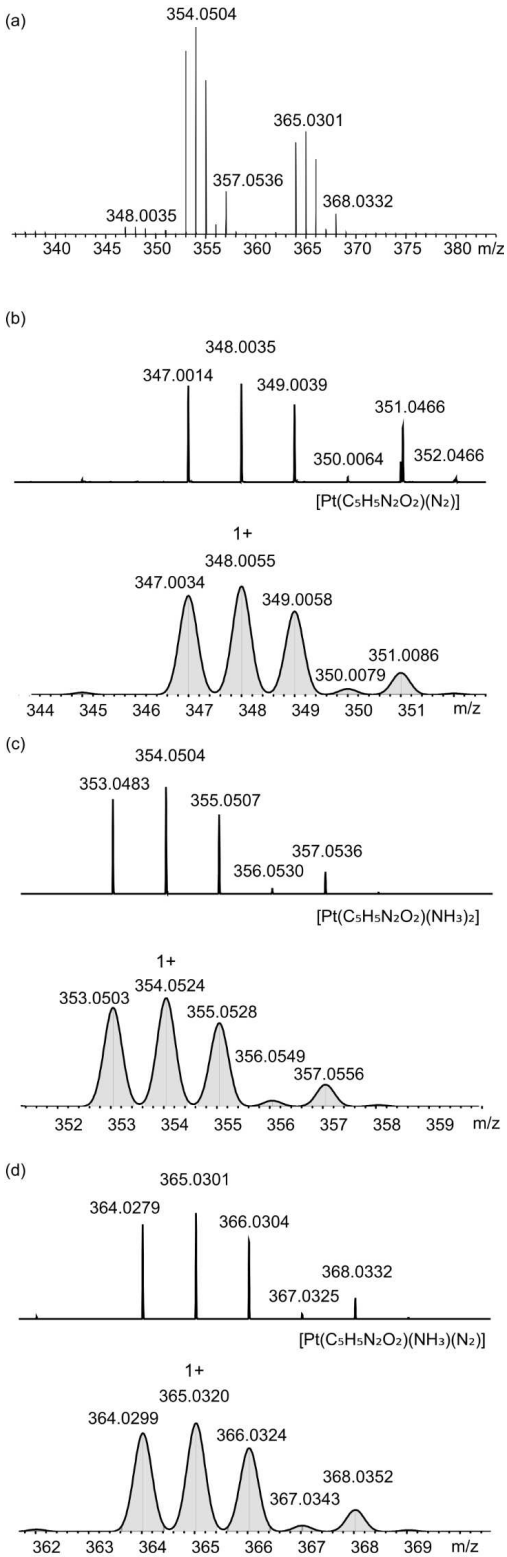

Figure 9. Section of experimental ESI-mass spectrum (a) and details of signals at *m/z* 348, 354, and 365 in sample (III) (b)-(d). Simulations are for $[Pt(1MeU)(N_2)]^+$, $[Pt(NH_3)_2(1MeU)]^+$, and $[Pt(NH_3)(1MeU)(N_2)]^+$.

The second most intense group of mass peaks occurs between ca. *m/z* 660 and *m/z* 770. They are attributed to species of $Pt_2(1MeU)_2$ stoichiometry. Relative intensities of these signals differ in dependence of sample history. While in samples (I) and (II) *m/z* 770 is the dominant one and assigned to $[Pt^{II}_2(NH_3)_4(1MeU)_2(NO_3)]^+$ (*head-tail* dimer **4**, possibly mixed with a small amount of *head-head* dimer **5** (c.f. NMR discussion), in sample (III) the most intense signal in this range occurs at *m/z* 726 (Figure S11). The latter is attributed to $[Pt^{II}_2(NH_3)_3(1MeU)_2(Cl)]^+$. Loss of NH_3 generates *m/z* 709. On the other hand, the *m/z* 725 signal in sample (I) is best simulated by composition $[(NH_3)_2(1MeU)Pt(\mu\text{-}OH)Pt(1MeU)(NH_3)_2]^+$, hence points to the presence of **3**. This difference in mass spectra is also reflected in the ^1H NMR spectra (see above). Loss of one NH_3 ligand from **4** (or **5**) gives $[Pt^{II}_2(NH_3)_3(1MeU)_2(NO_3)]^+$ (*m/z* 753), and loss of NH_3 from cation **3** leads to $[Pt^{II}_2(NH_3)_3(1MeU)_2(OH)]^+$ with *m/z* 708. A further loss of an ammonia ligand is expected to give rise to a signal at *m/z* 691. Such a signal is indeed observed with sample (III), yet not with sample (I). However, with (I) a weak signal is found at *m/z* 345.5, which manifests itself as being due to a +2 cation. We propose that it originates from a mixed-valence species, namely $[[Pt^{II}Pt^{III}(NH_3)_2(1MeU)_2(OH)]^{2+}$. The second most intense signal in sample (I) in this range is at *m/z* 690. Contrary to intuition, that it may arise from the μ-oxido derivative of the former $Pt^{II}Pt^{III}$ species following deprotonation of the OH^- group, simulation gives the best agreement for a composition $[Pt^{II}_2(NH_3)_2(1MeU)_2(NH_2)]^+$ (Delta 0.0040).

A closer look at the experimental signals reveals that in numerous cases the main signals are superimposed by one or more sets of low intensity which have their maxima at slightly different values (higher or lower), sometimes approaching less than one mass unit. We shall illustrate this feature in two representative cases (Figures 10 and 11).

In sample (II) the signal centered at *m/z* 708 is superimposed by a weaker signal centered at *m/z* 709, whereas in sample (III) relative intensities of the two sets are reversed. Simulations suggest that that *m/z* 708 corresponds to $[Pt^{II}_2(NH_3)_3(1MeU)_2(OH)]^+$, while *m/z* 709 originates from $[Pt^{II}_2(NH_3)_2(1MeU)_2(Cl)]^+$, with deviations from simulated masses being very small, 0.0003 and 0.0005 mass units, respectively. It is likely, that the signal at *m/z* 708 originates from **3** with loss of a NH_3 ligand. Similarly, the species with *m/z* 709 could be formed through loss of an ammonia ligand from *m/z* 726. A similar reversal in relative intensities is seen with the peaks centered at *m/z* 726 (major signal in (III)) and at *m/z* 725 (major signal in (I)) (not shown). Excellent agreement is achieved with simulations for $[Pt^{II}_2(NH_3)_3(1MeU)_2(Cl)]^+$ and $[Pt^{II}_2(NH_3)_4(1MeU)_2(OH)]^+$ (**3**), respectively.

A case, where the masses of two different species are nearly identical, is observed near *m/z* 743 in sample (III) (Figure 11). The dominant signal at *m/z* 743.0732 is best simulated by $[Pt^{II}_2(NH_3)_4(1MeU)_2(Cl)]^+$ (deviation 0.0006 mass units), while the minor one having a maximum peak at *m/z* 743.1150 points to a composition of $[Pt^{II}_2(NH_3)_4(1MeU)_2(OH)(OH_2)]^+$ (deviation 0.0027 mass units). $^-$The dinuclear compound in higher abundance could either be a μ-Cl^- complex or a complex with a single 1MeU bridge, whereas the minor species could be a pair of mononuclear hydrogen-bonded $OH_2\cdots OH^-$ entities, hence **1b·1b′**.[43]

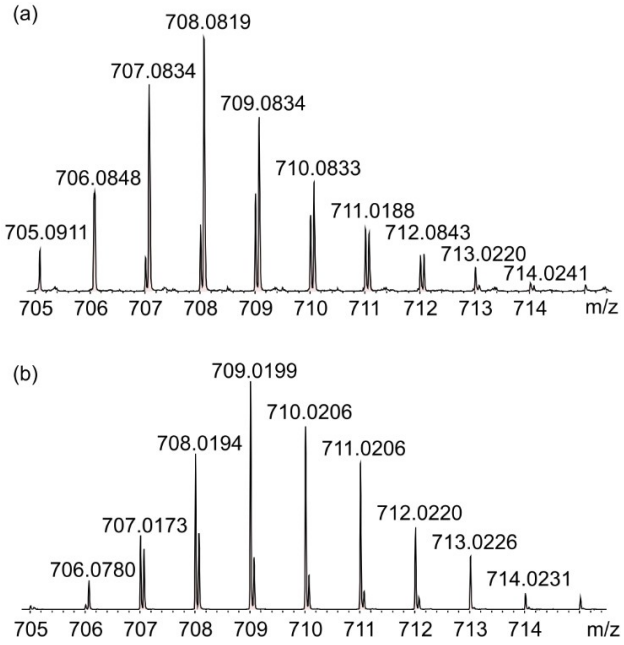

Figure 10. Sections of mass peaks at m/z 708 and 709 in (a) sample (II), and (b) sample (III). Relative intensities of individual isotopic lines are reversed in the two samples.

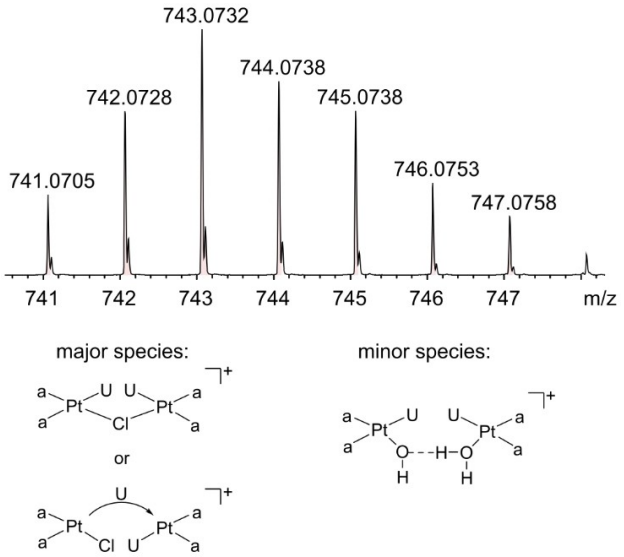

Figure 11. Overlapping signals at m/z 743 and proposed structures based on mass simulations.

The signal set centered at *m/z* 690 in sample (I) is of comparable intensity to that at *m/z* 770. Simulations suggest that it is due to $[Pt^{II}_2(NH_3)_2(1MeU)_2(NH_2)]^+$ (deviation 0.0059 mass units). A weak signal set observed at *m/z* 673 is assigned to $[Pt^{II}_2(NH_3)(1MeU)_2(NH_2)]^+$ (deviation 0.0012 mass units).

Two more species seem to be related to the latter species, both having a +2 charge: The signals centered at *m/z* 337 are

possibly due to $[Pt^{II}_2(NH_3)_2(1MeU)_2]^{2+}$ and those of *m/z* 328.5 due to $[Pt^{II}_2(NH_3)(1MeU)_2]^{2+}$.

Peaks with *m/z* values for +1 cations in the range 850–1300 are rather weak in all samples. Their exact compositions are increasingly difficult to determine, including the formal oxidation states of Pt. For example, *m/z* 852 and *m/z* 973 have been simulated for possible $Pt_2(1MeU)_3$ and $Pt_3(1MeU)_2$ stoichiometries, respectively, and different combinations of Pt oxidation states, for $Pt^{II}_2Ag(1MeU)_3$, as well as for $Pt^{IV}_2(1MeU)_4$. In the case of *m/z* 973 the best accuracy value was obtained for the option $[Pt^{IV}_2(1MeU)_4(NH_3)_2(NH_2)_2(OH)]^+$, hence a dinuclear Pt^{IV} oxidation product of **2**. This proposal is attractive in that it could involve two $[H_2NH\ldots NH_2]^-$ bridges as previously observed in dinuclear, mixed ammonia/amido complexes of Pt^{IV}.[44] (Figure S12). This proposal is further supported by the fact that the number of isotopic lines of this signal is inconsistent with a trinuclear Pt species and rather points to a compound containing two Pt atoms only.

The signals around *m/z* 1100 almost certainly refer to compounds of $Pt_3(1MeU)_3$ stoichiometries. The most intense one at *m/z* 1114 (in sample (II)) is reasonably well simulated by $[Pt^{III}_2Pt^{II}(1MeU)_3(NH_3)_3(NH_2)_2Cl_2]^+$, but the deviation is larger, 0.0726 mass units. The adjacent set at *m/z* 1097 is assigned to a species that has one NH_3 ligand less. *m/z* 1133 is well simulated by composition $[Pt^{II}_3(1MeU)_3(NH_3)_6Cl_2]^+$. The signal at *m/z* 1107 in the sample prepared with an excess of $AgNO_3$ is of identical $Pt_3(1MeU)_3$ stoichiometry, but the composition, including the Pt oxidation states, is different: $[Pt^{III}Pt^{II}_2(1MeU)_3(NH_3)_3(NH_2)_2(NO_3)]^+$ (deviation 0.0035 mass units). All these signals again display low-intensity sets of signals at closely similar masses.

The +1 ions with largest masses are detected at *m/z* 1258 and 1276. Their intensities are weak and they are assigned to compounds of $Pt_4(1MeU)_3$ stoichiometries with uncertainties regarding the other co-ligands.

As to differences in MS spectra between samples of **1a** treated with sub-stoichiometric amounts of $AgNO_3$ or an excess, expectedly a signal set due to $\{Na[Pt(NH_3)(1MeU)Cl]\}^+$ (*m/z* 395) is present in the sample treated with 0.8 equiv. of $AgNO_3$, yet it is missing in the sample reacted with 1.2 equiv. of $AgNO_3$ for three days.

Regarding the existence of μ-NH_2 species of Pt^{II}, we admit that it is essentially postulated based on the MS data. In the ^1H NMR spectra (D_2O) the NH_2 resonances are expected in the 2–3 ppm-range,[20] but their expected splitting in two components, their low abundance, and isotopic exchange reactions may explain why such resonances are not unambiguously observed.

Our attempts to identify Ag complexes or heteronuclear $Pt_xAg_y(1MeU)_z$ compounds in the MS spectra of the sample prepared with an excess of $AgNO_3$ (sample (I)) were only partly successful. Specifically, neither signals to be assigned to $[Ag(NH_3)_2]^+$, $\{[Pt(NH_3)_2(1MeU)Cl]Ag\}^+$, $\{[Pt(NH_3)_2(1MeU)_2]Ag\}^+$ (**2a**), nor $\{[Pt(NH_3)_2(1MeU)_2]_2Ag\}^+$ were detected. However, in the mass spectrum of (III) two weak signals originating from +1 cations are observed at *m/z* 480 and 497, the isotopic pattern of which strongly suggest that they are mixed Pt^{II},Ag complexes. The latter signal is also found in the mass spectrum of sample (I). Both main peaks are accompanied by two and three sets of very low intensity signals, respectively (Figure S13). Simulations suggest compositions of $[PtAg(NH_3)(1MeU)(OH)(OH_2)]^+$ for the main peak centered at *m/z* 480, and of $[PtAg(NH_3)_2(1MeU)(OH)(OH_2)]^+$ for the main peak at *m/z* 497.

2.6. N_2 Complexes Seen in the MS Study

Certainly, one of the great surprises of the mass spectra was the observation of the mentioned signals at *m/z* 365 and *m/z* 348, which we assign to $[Pt(NH_3)(1MeU)(N_2)]^+$ and $[Pt(1MeU)(N_2)]^+$, respectively. We tend to believe that they are formed during the ESI-MS experiment through reaction of a coordinatively unsaturated $[Pt(NH_3)(1MeU)]^+$ ion with the nitrogen dry gas rather than during the evaporation process of the sample synthesis via N_2 uptake from air, oxidation of coordinated NH_3, or a conproportionation reaction between NH_3 and any NO_x species or nitrate. Formation of a dinitrogen complex of Ru^{II}-N_2 complex under ESI-TOF mass spectroscopy conditions, likewise, believed to occur in the presence of the flow of the drying gas N_2, has been reported before.[45]

2.7. Products Formed Between 1b and *cis*-$[Pt(NH_3)_2(OH_2)_2]^{2+}$: Clear Evidence of Formation of $[NH_4]^+$

In a recent publication we have reported, among others, on the two major species formed between the above two components (2:1-ratio, D_2O) over a period of 3–6 weeks.[4] These are the self-condensation product **4**, hence the *head-tail* dimer, and also a dinuclear co-condensation product, namely *cis*-$[(NH_3)_2Pt(\mu\text{-}OH)(\mu\text{-}1MeU\text{-}N3,O4)Pt(NH_3)_2]^{2+}$ (**8**). A considerable number of very weak signals, mostly correlated by $^1H,^1H$-COSY, yet not assigned, account to only ca. 2–5% of total 1MeU signal intensity. We have now repeated this experiment and have modified it by reacting the components in a 1:1-ratio in H_2O, allowing the solution to evaporate to dryness in air, and subsequently recording ^1H NMR spectra (D_2O) of the redissolved blue material (H_2O; pH 4; maximum absorptions at 670 nm, minor one at 520–550 nm). Again, both a concentration- and time-dependence of NMR resonances is observed. It appears that the only common feature is the presence of three major species, namely **1b**, **4**, and **8**. While we are still unable to assign the many previously observed minor resonances in the ^1H NMR spectra, we have seen a number of new details which we would like to present in the following.

First, a species with unusual 1MeU proton shifts: Figure 12 gives views of H5 and H6 resonances of a dilute sample which had been brought to dryness prior to dissolving it in D_2O. The initially blue solution becomes purple within a day and eventually (1 week) has largely lost its color again. The region of H5 resonances reveals at least seven doublets. The three most intense ones are assigned to **4**, **1b**, and **8** (in decreasing order). There are in addition three doublets of moderate intensities, as well as a weak one, which overlaps with **4** and is tentatively assigned to **5**. Six of the H6 doublets can be readily correlated. Two additional doublets, at 7.08 and 7.82 ppm, display unusual

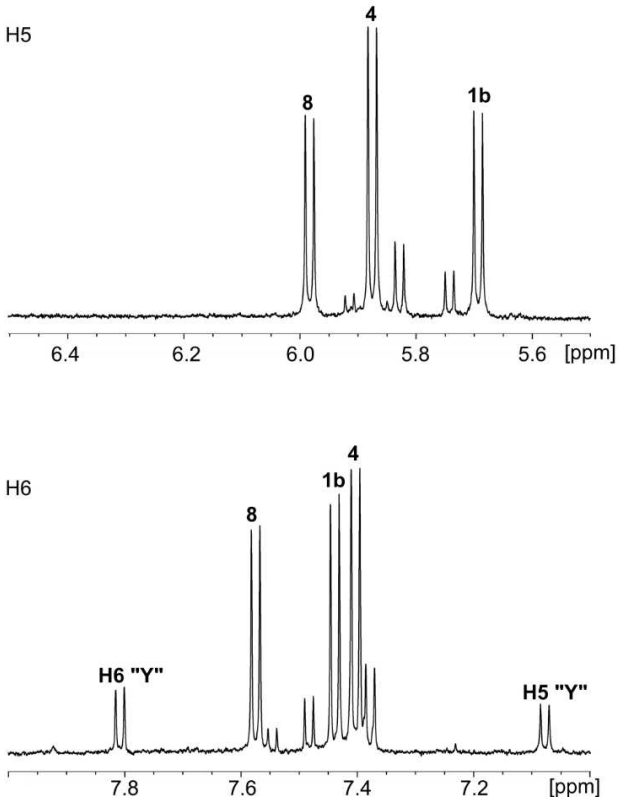

Figure 12. H5 and H6 resonances of 1MeU ligands present in a sample prepared as follows: Reaction of **1 b** with *cis*-$[Pt(NH_3)_2(OH_2)_2]^{2+}$ in a 1:1-ratio, evaporation to dryness in air, and dissolved in D_2O (1 mg in 1 mL). Only the three major species and species "Y" are assigned.

chemical shifts as compared to the others, and so does the CH_3 signal at 3.44 ppm. COSY spectroscopy (not shown) reveals that the two aromatic protons are coupled, and we assign them to H5 and H6 resonances of a 1MeU ligand. While the signal at lowest field is in the range expected for *head-tail* dinuclear diplatinum(III) compounds,[46] the shift of the H5 resonance is far off. We therefore tentatively assign these resonances to a 1MeU species **"Y"** of unknown composition which has a Pt^{II} ion at its N3 position and a second Pt ion at O4 oriented in such a way as to point toward the proton at the 5-position. This proposal is primarily based on the good agreement in chemical shifts with similar Pt^{II}-1MeU compounds adopting a "face-back" arrangement.[47,48] Within a week the distribution of the three main products undergoes changes similar to the ones discussed already, in that **1 b** becomes dominant (ca. 60% of complete intensity) over **4** and **8**, as well as **"Y"**.

Second, the appearance of resonances due to NH_4^+ and of metalorganic C5-platinated species: Although easily to be overlooked in the spectra discussed above, we noticed the growth of initially very weak resonances of a 1:1:1-triplet characteristic of NH_4^+ with time. In a more concentrated sample they are clearly discernable, appearing at ca. 7.05, 7.15, and 7.25 ppm as a consequence of proton coupling with ^{14}N. The three signals represent overlays of isotopomers of mixed $^1H,^2D$ species of the ammonium ions and consequently appear as relatively broad, fine-structured resonances.[49] There is a problem of identifying these resonances in the beginning because they are dispersed among a number (up to 10) of singlets of weak to moderate intensity between 6.5 and 7.3 ppm, yet they are clearly seen at a later stage (Figure 13 (b)).

As to the mentioned singlets, it is proposed that all of these singlets represent species with Pt being bonded to both N3 *and* C5. The Pt entity bonded to C5 originates from the added Pt-diaqua species. Typically, the H6 proton of C5-platinated 1MeU complexes are expected in this range, but unlike in spectra recorded with low-field instruments, ^3J coupling between the ^{195}Pt isotope and H6 is not observed in the present case (500 MHz).[50,51] A NOESY experiment (*N*uclear*O*verhauser*E*ffect-*S*pectroscop*Y*) indeed reveals a spatial closeness of these H6 singlets to those of the methyl protons at N1, thereby supporting our proposal (Figure 14). Clearly, the methyl resonances of the N3,C5-diplatinated compounds (3.28–3.37 ppm) are slightly upfield from those carrying Pt exclusively at N3. The sheer number of N3,C5-diplatinated species surprises at first glance, but it must be kept in mind that each of the identified 1MeU species, notwithstanding the unassigned ones, could have undergone platination reactions at the C5 position of uracil ligands, thereby generating a multitude of products. It

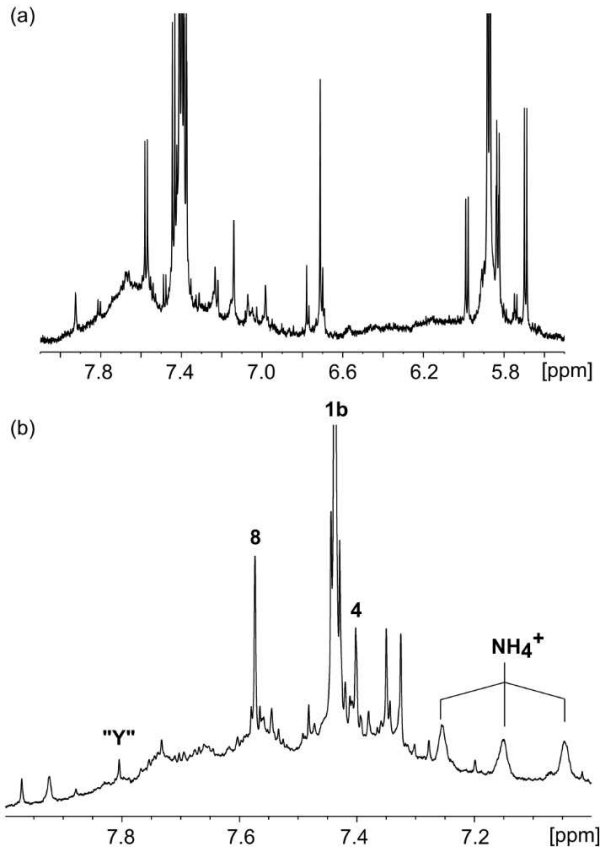

Figure 13. (a) H5 and H6 resonances (D_2O, 500 MHz, 30 mg/0.7 mL, DSS) of products obtained upon reaction of **1 b** with *cis*-$[Pt(NH_3)_2(OH_2)_2]^{2+}$ (1:1) and evaporation to dryness, immediately after dissolving in D_2O. The solution is blue-black. (b) H6 resonances of identical sample, 4 months after spectrum (a). Due to H–D exchange of the H5 protons, the original H6 doublets appear largely as singlets. The 1:1:1-triplet of NH_4^+ (and $NH_xD_y^+$) is clearly discernible.

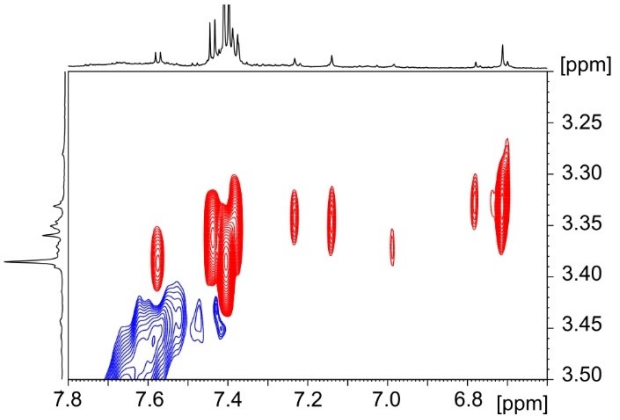

Figure 14. Section of NOESY spectrum of sample shown in Figure 14 (a), illustrating the cross-peaks of the H6 singlets in the shift range 6.6–7.3 ppm with CH_3 singlets.

appears that the formation of N3,C5-diplatinated compounds and the generation of free NH_4^+ are interrelated, possibly as a consequence of a trans-effect of the C5 bound nucleobase.[50] Formation of NH_4^+ in complicated mixtures of *cis*-$Pt^{II}(NH_3)_2$ and 1MeUH has previously been noted by us and in fact has been quantified.[3]

With time (months), the following changes occur: The major species, **1 b**, **8**, and **4**, have undergone almost complete isotopic exchange of their H5 resonances, leading to pseudo-"triplets" of H6 and the disappearance of the original H5 doublets. Two H6 singlets at 7.35 and 7.33 ppm, which approach the intensity of **4**, remain, but most of the other singlets between 6.5 and 7.3 ppm, attributed to N3,C5 Pt_2 compounds, have disappeared or have become very weak (Figure 13 (b)).

Third, there is a broad "bump" which superimposes the individual H6 resonances and presumably is caused by paramagnetic oligomers. Moreover there are also a number of isolated singlets at low field, e.g. at 7.92 and 7.97 ppm, which likewise are unaccounted for (Figure 13 (b)). All we can exclude is that these resonances are due to a C5-C5'-diuracil product earlier obtained by us during the reaction of 1MeUH with $[AuCl_4]^-$.[53]

Fourth, in several cases, but most pronounced in the NMR experiment described above, we noticed the gradual appearance of a new sets of signals derived from the internal DSS reference, which occur slightly downfield from DSS. See also Exp. Section.

2.8. Preparative Work: *trans*-$[Pt(NH_3)(1MeU\text{-}N3)I_2]^-$ and its Solution Chemistry

Our earlier applied procedure to convert *cis*-$[Pt(NH_3)_2(1MeC\text{-}N3)Cl]Cl$ into *trans*-$[Pt(NH_3)(1MeC\text{-}N3)I_2]$ (and likewise the corresponding 9-ethylguanine and 9-methyladenine analogues[54]) by treating the starting compound with KI at acidic pH to release one of the two ammonia ligands as an ammonium ion,[2] was not particularly successful in the present case, starting from **1 a**, presumably as a consequence of the very poor water-solubility of the iodo analogue **1a'** which requires high temperatures to react, combined with the sensitivity of the Pt-(1MeU-*N3*) bond toward H^+. A modification of the above procedure – addition of DMSO to the aqueous solution of **1 a** prior to addition of KI – did not improve the yield markedly. Even though *trans*-$[Pt(NH_3)(1MeU\text{-}N3)I_2]^-$ was eventually isolated as Cs^+ (**9**) and $[Pt(NH_3)_4]^{2+}$ salts (**10**),[28] the main product was unreacted **1a'**. Formation of $[Pt(NH_3)_4]^{2+}$ can be rationalized according to

$$3\ \textit{cis}\text{-}[Pt(NH_3)_2(1MeU)Cl] + 4\ KI =$$
$$2\ \textit{trans}\text{-}[Pt(NH_3)_2(MeU)I_2]^- + [Pt(NH_3)_4]^{2+}$$
$$+K(1MeU) + 3\ KCl$$

with the possibility of a DMSO intermediate playing a role in the overall reaction. A DMSO-containing side product, *trans*-$[Pt(NH_3)(DMSO\text{-}S)I_2]$ (**11**), has indeed been isolated and structurally characterized in a reaction performed under somewhat modified conditions (see Experimental Section and Supporting Information).

The crystal structure of $Cs[Pt(NH_3)(1MeU\text{-}N3)I_2]\ 4H_2O$ (**9**) has been reported by us previously.[28] The cation and the anion of $[Pt(NH_3)_4][trans\text{-}Pt(NH_3)(1MeU\text{-}N3)I_2]_2 \cdot 5H_2O$ (**10**) are depicted in Figure 15. The atom numbering scheme is given for the asymmetric unit. Different to the situation with **1a'**, the 1MeU ligand is nearly perpendicular (86.0(3)°) to the Pt coordination plane. Pt–N and Pt–I bond lengths (Table S2) are close to those of **1a'**, **9**, and *trans*-$K_2[Pt(1MeU\text{-}N3)_2I_2]$[28a], taking into consideration the structural trans-effect of iodide ligands. While in **9**, where Cs^+ ions cross-link *trans*-$[Pt(NH_3)(1MeU\text{-}N3)I_2]^-$ anions to produce a coordination polymer, in compound **10** there is an extensive hydrogen bond network between the NH_3 ligands of the cations and the O4 as well as O2 acceptors of the anions and to the crystal water. In addition, the NH_3 ligand of the anion forms a hydrogen bond with O4 of a neighboring anion and also with the crystal water (Figures S14).

Both ^1H and ^{195}Pt NMR spectra of **9** in D_2O reveal the presence of two species in a ratio of 7:1. The ^{195}Pt NMR shifts of −3283 (major species) and −3351 ppm (minor one) are too close to assume that one of these represents a hydrolysis species of the other.[55] Since both signals are in the range expected for species with PtN_2I_2 coordination spheres, we rather propose that the minor species is due the cis isomer of **9**,

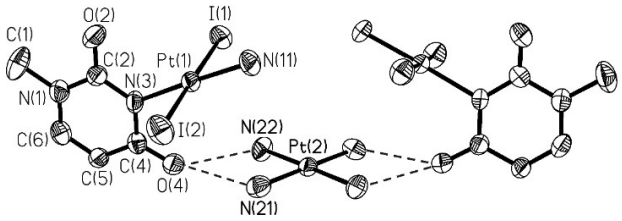

Figure 15. X-ray crystal structure of the cation and anion of $[Pt(NH_3)_4][trans\text{-}Pt(NH_3)(1MeU\text{-}N3)(I)_2]_2 \cdot 5H_2O$ (**10**) with atom numbering scheme of the asymmetric unit. Ellipsoids are drawn at the 50% probability level. The Pt2 atom sits on a center of symmetry and the second half of the complex salt is generated by the symmetry operation -x+1,+y,-z+1.5.

formed under the harsh conditions of the preparation and admixed with the trans isomer in the solid recovered. Elemental analysis, which agrees with the composition established by X-ray analysis, of course cannot rule out the presence of a second isomer.

Treatment of **9** with 2 equiv. of $AgNO_3$ in D_2O (0.02 M, pD 2.6) produces a yellow solution with major 1MeU doublets at 7.42 ppm (H6) and 5.68 ppm (H5) which we assign to *trans*-$[Pt(NH_3)(1MeU\text{-}N3)(OD_2)_2]^+$ (**1e**). Within hours, the solution adopts an intense blue color with and within days the sample develops broad bumps (0.4 ppm wide) of unstructured resonances at the lowfield sides of H5 and H6 resonances. After three days a strong absorption band at 537 nm and a shoulder at 640 nm are observed in the UV/vis spectrum. The resonances assigned to **1e** and present from the beginning can still be seen, but are subject to gradual isotopic exchange of the H5 protons. There are in addition two minor sets of sharp doublets (H5: 5.90 and 5.78 ppm; H6: 7.59 and 7.35 ppm). We are unable to properly assign these two sets at present, but would like to point out that within the related $[Pt(NH_3)(1MeC\text{-}N3)(OD_2)_2]^{2+}$ system we have observed two isomeric *head-tail* dimers of composition $[Pt_2(NH_3)_2(OD_2)_2(\mu\text{-}1MeC_{-H}\text{-}N3,N4)_2]^{2+}$, depending on the relative positions of NH_3 with respect to N3 of 1MeC (cis or trans).[2] Their ^1H NMR resonances are very similar and also do not differ much from the corresponding *head-tail* dimer derived from *cis*-$[Pt(NH_3)_2(1MeC\text{-}N3)(OD_2)]^{2+}$, very much as in the present situation. If the analogy of cis- and trans-isomers of $[Pt(NH_3)(1MeU\text{-}N3)(OD_2)_2]^+$ with that of the corresponding 1MeC complexes (charge +2) holds also with respect to the differential oxidizability of the *head-tail* dinuclear derivatives, then one might indeed expect rapid partial oxidation of the condensation product of *trans*-$[Pt(NH_3)(1MeU\text{-}N3)(OD_2)_2]^+$ in the presence of air. Whether or not an association beyond the dinuclear level takes place (with additional involvement of O2 sites of the 1MeU ligands), remains unclear.[56]

3. Conclusions

Despite their marked differences in sensitivity, the combined applications of ^1H NMR spectroscopy and ESI mass spectrometry on species derived from the simple model nucleobase complex *cis*-$[Pt(NH_3)_2(1MeU\text{-}N3)Cl]$ (**1a**) has helped us greatly to better understand the complex solution chemistry of its hydrolysis product **1b**. First, the solution behavior of **1a** in water is relatively unspectacular. It includes hydrolysis of the chloride ligand, formation of the μ-OH complex **3**, partial NH_3 loss as a consequence of the kinetic trans effect of Cl^-, as well as formation of secondary hydrolysis products. In gas phase (conditions of ESI-MS experiment) association of neutral **1a** via Na^+ ions appears to be common. Second, removal of Cl^- from **1a** by means of $AgNO_3$ is anything but a reaction going to completion. Initially **1a** forms a soluble heteronuclear complex with Ag^+, and heteronuclear derivatives of Pt condensation products are detectable by ESI-MS. There exists the possibility that AgCl becomes solubilized by Pt coordination complexes, as previously observed by us.[57] Third, the solution behavior of **1b**, alone or in the presence of **1a** or any of the other feasible species **1c**–**1e**, is very complex. Different ways of condensation reactions *and* their co-existence are responsible for the observed multitude of products, which differ in size *and* ligand bridging modes. The latter may involve OH^-, $1MeU^-$, Cl^-, and NH_2^- or combinations thereof. The positioning of the other, non-bridging ligands (possibility of diastereomer formation) and differences in Pt oxidation states (possibility of mixed-valency) adds to the complexity. For dinuclear compounds of $Pt_2(1MeU)_2$ stoichiometry, ESI-MS has revealed 12 different variants. Among these, four dinuclear species have retained their four NH_3 ligands. The others are short in NH_3, or ammonia ligands have become amido ligands. Resonances of the μ-amido ligands have not been unambiguously detected by ^1H NMR spectroscopy in the expected shift range of 2–3 ppm.[20] The largest mass detected by ESI-MS is that of a $Pt_4(1MeU)_3$ stoichiometry. Fourth, the diaqua species *cis*-$[Pt(NH_3)_2(OH_2)_2]^{2+}$, when present, not only condenses with **1b** to give compound **8**, but in concentrated solutions also to N3,C5-diplatinated compounds. It appears that the generation of $[NH_4]^+$ as seen in the ^1H NMR spectra, is a consequence of Pt binding to C5 of the uracil ligand. Fifth, both partially oxidized Pt compounds and Pt^{IV} species are formed with time. Since none of the mixed-valence compounds was isolated, the question regarding the origin of the sample colors observed, cannot be answered. However, the absorption spectra recorded are inconsistent with that of the well-known tetranuclear $Pt^{2.25}$ complex of 1MeU. Sixth, sample treatment strongly affects product composition. Speciation in solution not only depends on concentration and pH, but also differs from that of samples brought to dryness prior to re-dissolving them. Even the way of solidification (evaporation in air *vs.* vacuum evaporation) makes a difference. This finding may also be relevant to conflicting reports on the composition of "Platinum Pyrimidine Blues" and their activity as antitumor drugs.

Experimental Section

Materials

cis-$[Pt(NH_3)_2(1MeU\text{-}N3)Cl]\cdot H_2O$ (**1a**) was prepared as described.[13] The corresponding iodide analogue *cis*-$[Pt(NH_3)_2(1MeU\text{-}N3)I]$ (**1a'**) was obtained as follows: To a solution of 1 mmol of **1a** in water (80 mL) was added 4 mmol of KI, the pH adjusted to 2–3 with HNO_3, and the mixture stirred for 48 h at 40 °C. Yellow crystals, filtered and washed with water, were then obtained in 88% yield. Elemental analysis calcd (%) for $C_{10}H_{11}N_4O_2I$ Pt: C 12.5, H 2.3, N 11.6; found: C 12.5, H 2.2, N 11.8.

The syntheses of *trans*-$Cs[Pt(NH_3)(1MeU\text{-}N3)I_2]\ 4H_2O$ (**9**) and $[Pt(NH_3)_4][trans\text{-}Pt(NH_3)(1MeU\text{-}N3)I_2]_2\cdot 5H_2O$ (**10**) have been reported.[28] Elemental analysis calcd (%) for $C_{10}H_{38}N_{10}O_9I_4Pt_3$ (**10**): C 7.8, H 2.5, N 9.1; found: C 7.8, H 2.5, N 9.1. ^1H NMR of **9** (D_2O, pD 7.5, DSS, δ, ppm): major species H6, 7.34 (d, ^3J 7.4 Hz), H5, 5.58 (d), CH_3, 3.32 (s), NH_3, 3.47 (s, broad); minor species H6 7.38 (d, ^3J 7.4 Hz), H5, 5.61 (d).

trans-$[Pt(NH_3)(DMSO\text{-}S)I_2]$ (**11**) was obtained as follows: **1a** and $AgNO_3$ (0.3 mmol each) were dissolved in a mixture of H_2O (10 mL) and DMSO (5 mL) and thae pH was brought to 3 by means of 0.1 N HNO_3. The mixture was stirred at 60 °C for 7d, with the pH

occasionally readjusted with HNO_3. After filtration of AgCl the filtrate was brought to dryness by rotary evaporation, and the colorless solid was dissolved in H_2O (10 mL). KI (0.75 mmol) was added and the mixture stirred for 3d at 40 °C. The resulting red precipitate of **11** was filtered, washed with water and dried in air. Storage of the filtrate at 4 °C for six weeks yielded an additional crop, which after recrystallization from water gave red crystals suitable for X-ray crystallography. The total yield of **11** was 20%. Elemental analysis calcd (%) for $C_2H_9NOSI_2Pt$: C 4.4, H 1.7, N 2.6; found: C 4.3, H 1.6, N 2.7. ^{1}H NMR (D_2O, pD 8.4): 3.87 ppm (s, CH_3); no indication of uncoordinated DMSO. As compound **11** is unrelated to the nucleobase complexes discussed in this paper, structural details are given in the Supporting Information only (Figure S15 and Table S3). Crystallographic data of **11** are included in Tables S1–S3.

The diaqua species of Cisplatin, used for the reaction with **1b**, was obtained by treating *cis*-[$Pt(NH_3)_2Cl_2$] with 2 equiv. of $AgNO_3$ with stirring in H_2O (24 h, 22 °C, daylight excluded) and subsequent centrifugation of AgCl.

Instrumentation

Elemental analysis data were obtained on a Leco CHNS-932 instrument. The ^{1}H NMR spectra were recorded in D_2O on Bruker 500 MHz AVANCE NEO and 600 MHz AVANCE III HD instruments. The ^{1}H,^{1}H-COSY and DOSY spectra were measured on the Bruker AV 500 AVANCE NEO instrument and the NOESY was performed on the 600 MHz Bruker AVANCE III HD. The ^{195}Pt NMR spectrum of compound **10a** in D_2O was recorded on a Bruker AC 200 spectrometer with K_2PtCl_6 as external reference. pD values of NMR samples in D_2O were measured by using a glass electrode and the addition of 0.4 units to the uncorrected pH value measured. Chemical shifts are referenced to sodium-3-(trimethylsilyl)propanesulfonate (DSS; 0 ppm). We note that we have repeatedly observed that the reference slowly (within weeks) developed a second minor set of resonances slightly downfield from those of DSS (see, eg. Figure S16). We can definitely exclude the possibility that this new set of resonances is due to the hydrolysis product 3-(trimethylsilyl)-1-propanol and, given the slow formation, formation of a Pt complex of DSS likewise seems unreasonable. UV/Vis spectra were recorded on a DAD HP-8453 UV-Vis spectrometer.

ESI-MS experiments were performed on BrukerESI-timsTOF (electrospray ionization-trapped ion mobility-time of flight) and Bruker compact high-resolution LC mass spectrometers (positive/negative mode). For calibration of the TIMS and TOF devices, Agilent ESI-Low Concentration Tuning Mix was applied. Simulations were made with Bruker Daltonics Data Analysis Software.

X-ray crystallography

Intensity data for **1a'**, **10**, and **11** were collected on an Enraf-Nonius-KappaCCD (Mo-K_α, $\lambda = 0.71069$ Å, graphite monochromator). Data processing was performed using DENZO and SCALEPACK.[58] The structures were solved by standard Patterson methods and refined by full-matrix least-squares based on F^2 using the SHELXTL PLUS[59] as well as SHELXL-93 programs.[60] All non-hydrogen atoms have been refined anisotropically, hydrogen atoms were added in calculated positions. Crystal data and data collection parameters are summarized in Tables S1 – S3.

CCDC-2038930 (**11**), 2038931 (**1a'**), 2038932 (**10**) contain the supplementary crystallographic data for this paper. These data can be obtained free of charge from The Cambridge Crystallographic Data Centre via www.ccdc.am.ac.uk/data_request/cif.

Acknowledgements

This work has been supported by TU Dortmund. We thank Prof. Dr. Guido Clever for providing facilities to carry out this work. We wish to also thank Prof. Dr. Michael Linscheid, Berlin, for helpful discussions, Dr. Oliver Janka, Münster, for carrying out the EDX measurements, and Laura Schneider for running the ESI-mass spectra.

Conflict of Interest

The authors declare no conflict of interest.

Keywords: 1-methyluracil · platinum · condensation reactions · NMR spectroscopy · mass spectrometry

[1] J. J. Wilson, S. J. Lippard, *Chem. Rev.* **2014**, *114*, 4470–4495.
[2] S. Siebel, C. Dammann, P. J. Sanz Miguel, T. Drewello, G. Kampf, N. Teubner, P. J. Bednarski, E. Freisinger, B. Lippert, *Chem. Eur. J.* **2015**, *21*, 17827–17843.
[3] S. Siebel, C. Dammann, W. Hiller, T. Drewello, B. Lippert, *Inorg. Chim. Acta* **2012**, *393*, 212–221.
[4] S. Pullen, W. G. Hiller, B. Lippert, *Inorg. Chim. Acta* **2019**, *494*, 168–180.
[5] J. P. Davidson, P. J. Faber, R. G. Fischer, Jr., S. Mansy, H. J. Peresie, B. Rosenberg, L. VanCamp, *Cancer Chemother. Rep.* **1975**, *59*, 287–300.
[6] K. A. Hofmann, G. Bugge, *Ber. Dtsch. Chem. Ges.* **1908**, *41*, 312–314.
[7] N. V. Cherkashina, D. I. Kochubey, V. V. Kanazhevskiy, V. I. Zaikovskii, V. K. Ivanov, A. A. Markov, A. P. Klyagina, Z. V. Dobrokhotova, N. Y. Kozitsyna, I. B. Baranovsky, O. G. Ellert, N. E. Efimov, S. E. Nefedov, V. M. Novotortsev, M. N. Vargaftik, I. I. Moiseev, *Inorg. Chem.* **2014**, *53*, 8397–8406.
[8] See, e.g.: a) J. K. Barton, H. N. Rabinowitz, D. J. Szalda, S. J. Lippard, *J. Am. Chem. Soc.* **1977**, *99*, 2827–2829; b) J. K. Barton, S. A. Best, S. J. Lippard, R. A. Walton, *J. Am. Chem. Soc.* **1978**, *100*, 3785–3788; c) T. V. O'Halloran, P. K. Mascharak, I. D. Williams, M. M. Roberts, S. J. Lippard, *Inorg. Chem.* **1987**, *26*, 1261–1270.
[9] See, e.g.: a) K. Sakai, K. Matsumoto, *J. Am. Chem. Soc.* **1989**, *111*, 3074–3075; b) K. Matsumoto, K. Sakai, K. Nishio, Y. Tokisue, R. Ito, T. Nishide, Y. Shichi, *J. Am. Chem. Soc.* **1992**, *114*, 8110–8118; c) C. H. Hendon, A. Walsh, N. Akiyama, Y. Konno, T. Kajiwara, T. Ito, H. Kitagawa, K. Sakai, *Nat. Commun.* **2016**, *7*, 11950.
[10] K. Umakoshi, T. Kojima, Y. H. Kim, M. Onishi, Y. Nakao, S. Sakaki, *Chem. Eur. J.* **2006**, *12*, 6521–6527.
[11] a) R. Uson, J. Forniés, M. Tomás, B. Menjón, K. Sünkel, R. Bau, *J. Chem. Soc. Chem. Commun.* **1984**, 751–752; b) E. S. Peterson, R. D. Larsen, H. E. Abbott, *Inorg. Chem.* **1988**, *27*, 3514–3518; c) E. Ambach, W. Beck, *Z. Naturforsch.* **1985**, *40b*, 288–291.
[12] B. Lippert, P. J. Sanz Miguel, *Acc. Chem. Res.* **2016**, *49*, 1537–1545.
[13] B. Lippert, D. Neugebauer, G. Raudaschl, *Inorg. Chim. Acta* **1983**, *78*, 161–170.
[14] H. Schöllhorn, U. Thewalt, B. Lippert, *J. Am. Chem. Soc.* **1989**, *111*, 7213–7221.
[15] H. Schöllhorn, U. Thewalt, B. Lippert, *Inorg. Chim. Acta* **1985**, *106*, 177–180.
[16] a) R. Faggiani, C. J. L. Lock, R. J. Pollock, B. Rosenberg, G. Turner, *Inorg. Chem.* **1981**, *20*, 804–807; b) U. Thewalt, D. Neugebauer, B. Lippert, *Inorg. Chem.* **1984**, *23*, 1713–1718.
[17] U. K. Häring, R. B. Martin, *Inorg. Chim. Acta* **1983**, *78*, 259–267.
[18] L. Schenetti, G. Bandoli, A. Dolmella, G. Trovó, B. Longato, *Inorg. Chem.* **1994**, *33*, 3169–3176 .
[19] a) W.-Z. Shen, B. Lippert, *J. Inorg. Biochem.* **2008**, *102*, 1134–1140; b) W.-Z. Shen, D. Gupta, B. Lippert, *Inorg. Chem.* **2005**, *44*, 8249–8258.
[20] L. Yin-Bandur, P. J. Sanz Miguel, L. Rodriguez-Santiago, M. Sodupe, M. Berghaus, B. Lippert, *Chem. Eur. J.* **2016**, *22*, 13653–13668.
[21] a) N. W. Alcock, P. Bergamini, T. J. Kemp, P. J. Pringle, S. Sostero, O. Traverso, *Inorg. Chem.* **1991**, *30*, 1594–1598; b) K. Matsumoto, K.

Harashima, *Inorg. Chem.* **1991**, *30*, 3032–3034 ; c) J. J. Wilson, S. J. Lippard, *Inorg. Chem.* **2012**, *51*, 9852–9864.
[22] A. Oksanen, M. Leskelä, *Acta Chem. Scand.* **1994**, *48*, 485–489, and refs. cited.
[23] B. Lippert, C. J. L. Lock, R. A. Speranzini, *Inorg. Chem.* **1981**, *20*, 808–813.
[24] See, e.g.: a) I. A. G. Roos, A. J. Thomson, J. Eagles, *Chem. Biol. Interactions* **1974**, *8*, 421–427; b) S. M. O. Quintal, Y. Qu, A. G. Quiroga, J. Moniodis, H. I. S. Nogueira, N. Farrell, *Inorg. Chem.* **2005**, *44*, 5247–5253; c) J. K.-C. Lau, D. Deubel, *P. Chem. Eur. J.* **2005**, *11*, 2849–2855; d) P. J. Sanz Miguel, M. Roitzsch, L. Yin, P. M. Lax, L. Holland, O. Krizanovic, M. Schürmann, E. C. Fusch, B. Lippert, *Dalton Trans.* **2009**, 10774–10786, and refs. cited.
[25] See, e.g.: a) S. Wherland, E. Deutsch, J. Eliason, P. B. Sigler, *Biochem. Biophys. Res. Commun.* **1973**, *54*, 662–668; b) D. Gibson, C. E. Costello, *Eur. Mass Spectrom.* **1999**, *5*, 501–510; c) V. Marchán, V. Moreno, E. Pedroso, A. Grandas, *Chem. Eur. J.* **2001**, *7*, 808–815; d) T. Hagemeister, M. Linscheid, *J. Mass Spectrom.* **2002**, *37*, 731–747; e) S. G. Hartinger, W. H. Ang, A. Casini, L. Messori, B. K. Keppler, P. J. Dyson, *J. Anal. At. Spectrom.* **2007**, *22*, 960–967; f) Y. Kasherman, S. Sturup, D. Gibson, *J. Biol. Inorg. Chem.* **2009**, *14*, 387–399; g) A. K. Boal, A. C. Rosenzweig, *J. Am. Chem. Soc.* **2009**, *131*, 14196–14197.
[26] J. Ruiz, M. D. Villa, V. Rodriguez, N. Cutillas, C. Vicente, G. López, D. Bautista, *Inorg. Chem.* **2007**, *46*, 5448–5449.
[27] A. Kashima, M. Sakate, H. Ota, A. Fuyuhiro, Y. Sunatsuki, T. Suzuki, *Chem. Commun.* **2015**, *51*, 1889–1892.
[28] Alkali ions binding to exocyclic O atoms of N(3) metalated 1MeU or 1MeT, see, e.g.: a) O. Renn, B. Lippert, I. Mutikainen, *Inorg. Chim. Acta* **1994**, *218*, 117–120; b) W. Micklitz, B. Lippert, F. Lianza, A. Albinati, *Inorg. Chim. Acta* **1994**, *227*, 5–10; c) F. Zamora, H. Witkowski, E. Freisinger, J. Müller, B. Thormann, A. Albinati, B. Lippert, *J. Chem. Soc. Dalton Trans.* **1999**, 175–182; d) E. Freisinger, A. Schneider, M. Drumm, A. Hegmans, S. Meier, B. Lippert, *J. Chem. Soc. Dalton Trans.* **2000**, 3281–3287.
[29] K. J. Koch, T. Aggerholm, S. C. Nanita, R. G. Cooks, *J. Mass Spectrom.* **2002**, *37*, 676–686.
[30] a) B. Fischer, H. Preut, B. Lippert, H. Schöllhorn, U. Thewalt, *Polyhedron* **1990**, *9*, 2199–2204; b) B. Pan, Y. Xiong, K. Shi, M. Sundaralingam, *Structure* **2003**, *11*, 825–831; c) Y. Ding, X. Wang, D. Li, W. Xu, *J. Phys. Chem. C* **2020**, *124*, 5257–5262.
[31] a) M. C. Wahl, M. Sundaralingam, *Trends Biochem. Sci.* **1997**, *22*, 97–102; b) A.-C. Uldry, J. M. Griffin, J. R. Yates, M. Pérez-Torralba, M. D. Santa Maria, A. L. Webber, M. L. Beaumont, A. Samoson, R. M. Claramunt, C. J. Pickard, S. P. Brown, *J. Am. Chem. Soc.* **2008**, *130*, 945–954.
[32] P. Hobza, J. Šponer, E. Cubero, M. Orozco, F. J. Luque, *J. Phys. Chem. B* **2000**, *104*, 6286–6292.
[33] see, e.g.: a) A. F. M. J. van der Ploeg, G. van Koten, K. Vrieze, *Inorg. Chem.* **1982**, *21*, 2026–2031; b) A. Albinati, K.-H. Dahman, A. Togni, L. M. Venanzi, *Angew. Chem.* **1985**, *79*, 760–761; c) R. Usón, J. Forniés, M. Tomás, J. M. Casas, F. A. Cotton, L. R. Falvello, *Inorg. Chem.* **1986**, *25*, 4519–4525; d) R. Usón, J. Forniés, M. Tomás, I. Ara, *Inorg. Chem.* **1994**, *33*, 4023–4028; e) T. Yamaguchi, F. Yamazaki, T. Ito, *J. Am. Chem. Soc.* **2001**, *123*, 743–744; f) V. G. Albano, M. Di Serio, M. Monari, I. Orabona, A. Panunzi, F. Ruffo, *Inorg. Chem.* **2002**, *41*, 2672–2677; g) M.-E. Moret, P. Chen, *J. Am. Chem. Soc.* **2009**, *131*, 5675–5690; h) J. Forniés, S. Ibáñez, E. Lalinde, A. Martín, M. T. Moreno, A. C. Tsipis, *Dalton Trans.* **2012**, *41*, 3439–3451; i) F. Liu, W. Chen, D. Wang, *Dalton Trans.* **2006**, 3015–3024, and refs. cited.
[34] a) B. Lippert, D. Neugebauer, *Inorg. Chim. Acta* **1980**, 46, 171–179; b) B. Lippert, H. Schöllhorn, U. Thewalt, *Inorg. Chem.* **1987**, *26*, 1736–1741; c) F. D. Rochon, R. Melanson, *Acta Crystallogr.* **1988**, *C44*, 474–477; d) W.-Z. Shen, R.-D. Schnebeck, E. Freisinger, B. Lippert, *Dalton Trans.* **2008**, 4044–4049.
[35] R. D. O'Sullivan, A. W. Parkins, N. W. Alcock, *J. Chem. Soc. Dalton Trans.* **1986**, 571–575.
[36] see, e.g.: a) B. R. Steele, K. Vrieze, *Transition Met. Chem.* **1977**, *2*, 169–174; b) D. P. Bancroft, F. A. Cotton, L. R. Falvello, W. Schwotzer, *Inorg. Chem.* **1986**, *25*, 763–770 ; c) B. Lippert, H. Schöllhorn, U. Thewalt, *Inorg. Chem.* **1987**, *26*, 1736–1741; d) E. Alonso, J. M. Casas, F. A. Cotton, X. Feng, J. Forniés, C. Fortuño, M. Tomas, *Inorg. Chem.* **1999**, *38*, 5034–5040; e) I. Aras, J. Forniés, C. Fortuño, S. Ibáñez, A. Martín, P. Mastrorilli, V. Gallo, *Inorg. Chem.* **2008**, *47*, 9069–9080.
[37] For removal of NH_3 from a mixed Pt,Ag complex, see: Y. Chikamoto, T. Kawamoto, A. Igashira-Kamiyama, T. Konno, *Inorg. Chem.* **2005**, *44*, 1601–1610.
[38] B. Lippert, P. J. Sanz Miguel, *Inorg. Chim. Acta.* **2016**, *327–328*, 333–348.
[39] T. V. O'Halloran, S. J. Lippard, *J. Am. Chem. Soc.* **1983**, *105*, 3341–3342.
[40] M. Krumm, I. Mutikainen, B. Lippert, *Inorg. Chem.* **1991**, *30*, 884–890.
[41] For equilibria between cyclic dimers and trimers, see, e.g.: a) J. M. Ludlow III, M. Tominaga, Y. Chujo, A. Schultz, X. Lu, T. Xie, K. Guo, C. N. Moorefield, C. Wesdemiotis, G. R. Newcome, *Dalton Trans.* **2014**, *43*, 9604–9611; b) M. Rancan, A. Dolmella, R. Seraglia, S. Orlandi, S. Quici, L. Armelao, *Chem. Commun.* **2012**, *48*, 3115–3117; c) E. Zangrando, M. Casanova, E. Alessio, *Chem. Rev.* **2008**, *108*, 4979–5013, and refs. Cited; d) B. Longato, D. Montagner, E. Zangrando, *Inorg. Chem.* **2006**, *45*, 8179–8187.
[42] A composition of $[Pt^{IV}(NH_3)_2(1MeU)(NO)(NO_3)]^+$ containing a nitroxyl anion and a chelating 1MeU or a chelating nitrate ligand would give a reasonable agreement, but is admittedly speculative.
[43] Transition metal complexes with M-OH…(OH_2)M bridges, see: a) M. Ardon, A. Bino, *Struct. Bonding* **1987**, *65*, 1–28; b) F. Lianza, A. Albinati, B. Lippert, *Inorg. Chim. Acta* **1997**, *255*, 313–318.
[44] L. Heck, M. Ardon, A. Bino, J. Zapp, *J. Am. Chem. Soc.* **1988**, *110*, 2691–2692.
[45] S. Masaoka, K. Sakai, *Chem. Lett.* **2009**, *38*, 182–183 (see Figure S6 in Supp. Inform.).
[46] H. Schöllhorn, P. Eisenmann, U. Thewalt, B. Lippert, *Inorg. Chem.* **1986**, *25*, 3384–3391.
[47] G. Frommer, F. Lianza, A. Albinati, B. Lippert, *Inorg. Chem.* **1992**, *31*, 243, 258–25604–2439.
[48] M. Höpp, A. Erxleben, I. Rombeck, B. Lippert, *Inorg. Chem.* **1996**, *35*, 397–403.
[49] W. McFarlane, R. R. Dean, *J. Chem. Soc. A* **1968**, 1535–1538.
[50] H. Schöllhorn, U. Thewalt, B. Lippert, *J. Chem. Soc. Chem. Commun.* **1986**, 258–260.
[51] L. Holland, W.-Z. Shen, W. Micklitz, B. Lippert, *Inorg. Chem.* **2007**, *46*, 11356–11365.
[52] M. Schmülling, A. D. Ryabov, R. van Eldik, *J. Chem. Soc. Dalton Trans.* **1994**, 1257–1263, and refs. cited.
[53] F. Zamora, P. Amo-Ochoa, B. Fischer, A. Schimanski, B. Lippert, *Angew. Chem.* **1999**, *111*, 2415–2417; *Angew. Chem. Int. Ed. Engl.* **1999**, *38*, 2274–2275.
[54] A. Hegmans, M. Sabat, I. Baxter, E. Freisinger, B. Lippert, *Inorg. Chem.* **1998**, *37*, 4921–4928.
[55] a) P. S. Pregosin, *Ann. Rep. on NMR Spectroscopy* **1986**, *17*, 285–349; b) T. G. Appleton, K. J. Barnham, J. R. Hall, M. T. Mathieson, *Inorg. Chem.* **1991**, *30*, 2751–2756.
[56] Any dimer-of-dimer formation to give Pt_4 species requires the association of *identical* enantiomers of the chiral *head-tail* species.
[57] A. Khutia, P. J. Sanz Miguel, B. Lippert, *Chem. Eur. J.* **2011**, *17*, 4205–4216.
[58] Z. Otwinowski, W. Minor, *Methods Enzymol.* **1997**, *276*, 307–326.
[59] G. M. Sheldrick, *Acta Crystallogr.* **1990**, *A46*, 467–473.
[60] G. M. Sheldrick, *SHELXL97*, University of Göttingen, Germany.

Manuscript received: October 29, 2020
Revised manuscript received: December 10, 2020